AD-A093 772 MISSION RESEARCH CORP ALBUQUERQUE NM F/G 20/14
AIRCRAFT EMP ISOLATION STUDY.(U)
JUL 80 A FINCI, H PRICE, P CHAO, S MERCER F29601-78-C-0082
UNCLASSIFIED AFWL-TR-79-156 NL

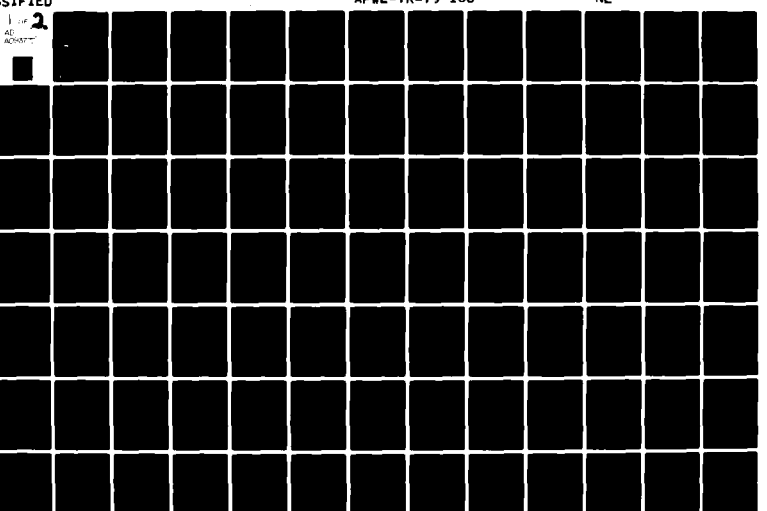

AFWL-TR-79-156

(2) LEVEL III

AD-E200630

AFWL-TR-79-156

AD A093772

AIRCRAFT EMP ISOLATION STUDY

A. Finci, et al.

Mission Research Corporation
1400 San Mateo Blvd., SE
Albuquerque, NM 87108

July 1980

Final Report

Approved for public release; distribution unlimited.

AIR FORCE WEAPONS LABORATORY
Air Force Systems Command
Kirtland Air Force Base, NM 87117

AFWL-TR-79-156

This final report was prepared by the Mission Research Corporation, Albuquerque, New Mexico, under Contract F29601-78-C-0082, Job Order 12090611 with the Air Force Weapons Laboratory, Kirtland Air Force Base, New Mexico. Mr Edsal H. Chappelle (NTMF) was the Laboratory Project Officer-in-Charge.

When US Government drawings, specifications, or other data are used for any purpose other than a definitely related Government procurement operation, the Government thereby incurs no responsibility nor any obligation whatsoever, and the fact that the Government may have formulated, furnished, or in any way supplied the said drawings, specifications, or other data, is not to be regarded by implication or otherwise, as in any manner licensing the holder or any other person or corporation, or conveying any rights or permission to manufacture, use, or sell any patented invention that may in any way be related thereto.

This report has been reviewed by the Public Affairs Office and is releasable to the National Technical Information Service (NTIS). At NTIS, it will be available to the general public, including foreign nations.

This technical report has been reviewed and is approved for publication.

EDSAL H. CHAPPELLE
Project Officer

FOR THE DIRECTOR

J. PHILIP CASTILLO, PhD
Chief, Electromagnetics Branch

THOMAS W. CIAMBRONE
Colonel, USAF
Chief, Applied Physics Division

DO NOT RETURN THIS COPY. RETAIN OR DESTROY.

UNCLASSIFIED

SECURITY CLASSIFICATION OF THIS PAGE (When Data Entered)

REPORT DOCUMENTATION PAGE		READ INSTRUCTIONS BEFORE COMPLETING FORM
1. REPORT NUMBER AFWL-TR-79-156 ✓	2. GOVT ACCESSION NO. AD-A093772	3. RECIPIENT'S CATALOG NUMBER
4. TITLE (and Subtitle) AIRCRAFT EMP ISOLATION STUDY		5. TYPE OF REPORT & PERIOD COVERED Final Report
		6. PERFORMING ORG. REPORT NUMBER
7. AUTHOR(s) A. Finci S. Mercer H. Price T. Naff P. Chao G. Simcox		8. CONTRACT OR GRANT NUMBER(s) F29601-78-C-0082
9. PERFORMING ORGANIZATION NAME AND ADDRESS Mission Research Corporation 1400 San Mateo Blvd., SE Albuquerque, NM 87108		10. PROGRAM ELEMENT, PROJECT, TASK AREA & WORK UNIT NUMBERS 64747F/12090611
11. CONTROLLING OFFICE NAME AND ADDRESS Air Force Weapons Laboratory (NTMF) Kirtland Air Force Base, NM 87117		12. REPORT DATE July 1980 ✓ 13. NUMBER OF PAGES 96
14. MONITORING AGENCY NAME & ADDRESS(if different from Controlling Office)		15. SECURITY CLASS. (of this report) Unclassified 15a. DECLASSIFICATION/DOWNGRADING SCHEDULE

16. DISTRIBUTION STATEMENT (of this Report)

Approved for public release; distribution unlimited.

17. DISTRIBUTION STATEMENT (of the abstract entered in Block 20, if different from Report)

18. SUPPLEMENTARY NOTES

19. KEY WORDS (Continue on reverse side if necessary and identify by block number)

Isolation
EMP
Aircraft
Aircraft Dielectric Stands

20. ABSTRACT (Continue on reverse side if necessary and identify by block number)

This report presents the results of a preliminary study into methods for electrically isolating the E-4B, the EC-135, and the EC-130 aircraft during EMP tests where the aircraft under test is directly driven by a high-voltage pulser.

DD FORM 1 JAN 73 1473

UNCLASSIFIED

SECURITY CLASSIFICATION OF THIS PAGE (When Data Entered)

CONTENTS

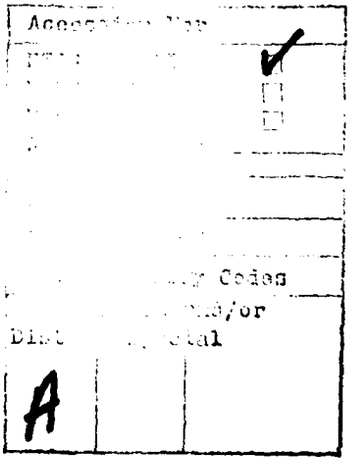

ILLUSTRATIONS

ILLUSTRATIONS (Continued)

TABLES

SECTION I
INTRODUCTION

This report presents the results of a preliminary study into methods for electrically isolating the E-4B, the EC-135, and the EC-130 aircraft during EMP tests where the aircraft under test is directly driven by a high-voltage pulser. Aircraft isolation is necessary to prevent the landing gear, engine nacelles, small antennas on the underside of the aircraft, and other protuberances from arcing to ground.

The means available to prevent arcing of the aircraft to ground are somewhat limited: for example, one can elevate the aircraft, alter the exterior of the aircraft in locations where the local electric field strength is excessive, replace the surrounding air with gas of a higher dielectric strength, or excavate portions of the ground under the aircraft. Indeed, the isolation methods investigated in the sequel utilize a combination of these techniques. Of course, it is not intended to prevent corona, since it occurs many places in flight. Here, it is only intended to prevent arcing from the aircraft to ground.

The proposed methods of isolating the aircraft are presented in the following section entitled, "Summary of Proposed Aircraft Isolation." The remainder of the report presents justification for these designs. For those readers unfamiliar with the physics and relationships used in breakdown analysis, sections have been included to explain the underlying physical processes.

Finally, we wish to point out that the analysis and designs presented in this report were performed by Physics International under subcontract to Mission Research Corporation.

During the course of this investigation, certain dimensions of the aircraft landing gear and antennas have been obtained, either by actual measurement, or by literature review. We have included an appendix in this report to document these dimensions.

SECTION II
SUMMARY OF PROPOSED AIRCRAFT ISOLATION

The purpose of this section is to present a brief summary of a proposed aircraft-isolation method to prevent flashover to ground of any portion of the aircraft, when exposed to a 3 megavolt, 1/50 (decay time constant), double-exponential waveform.

In order to accomplish this goal, it is necessary to elevate the aircraft on insulated pads constructed of alternate layers of dielectric and metal. The metallic layers serve to grade the voltage from the landing gear to ground. Figure 1 is an illustration of one of these pads showing the E-4B landing gear assembly and a metallic structure necessary to protect the tires. The details of this and another pad structure are contained in the following material.

In addition to elevating the aircraft on pads, it will be necessary to enclose all, or portions (depending on the aircraft) of, the underside of the aircraft with heavy (20 mil) polyethylene. The plastic is used to contain atmospheric-pressure Freon on the underside of the aircraft. The plastic is continuous across the ground, and fastened to the fuselage with tape. Figure 2, 3 and 4 show the E-4B, EC-135, and EC-130 aircraft on the pads, with the plastic in place.

To move the aircraft onto the pads, a ramp-bridge assembly is proposed. A sketch of this concept is shown in Figure 5 along with the E-4B aircraft. The method used to propel the aircraft onto the pads is not shown. The aircraft will be towed onto the pad structure by means of a cable. A winch or pulley arrangement powered either separately or by means of an aircraft tractor will be temporarily fastened to the nose-wheel end of the pad. After the aircraft is towed onto the pad, this structure can be easily removed.

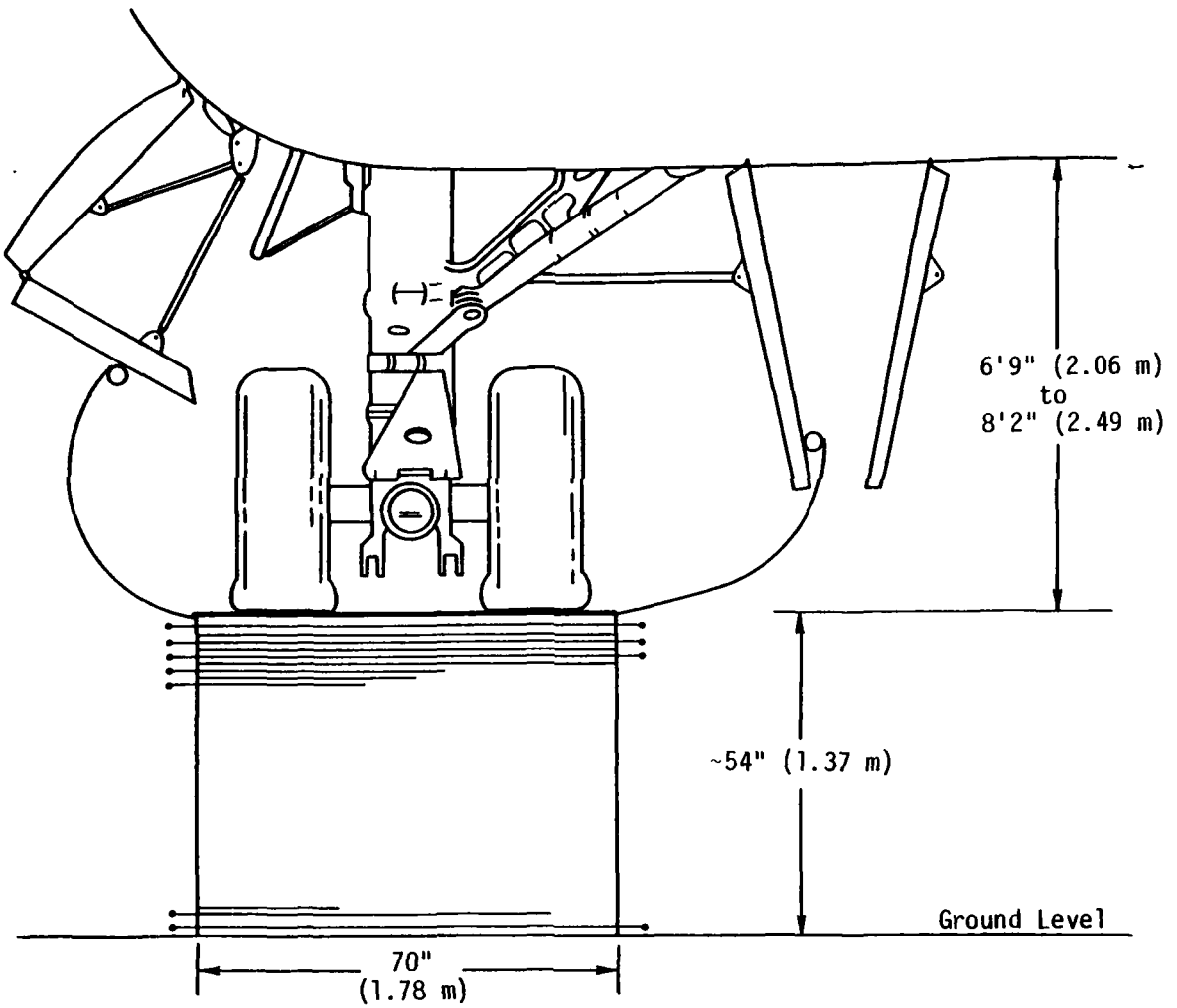

Figure 1. Laminated acrylic sheet (flat-type) stand shown with the E-4B main gear assembly.

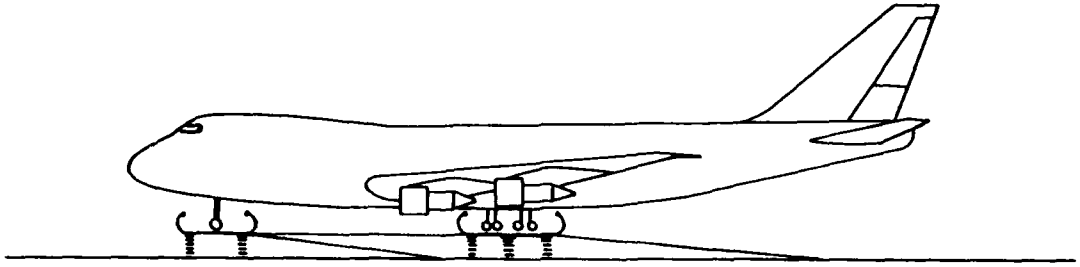

(a) Ramp/bridge assembly in place with top grading structure added.

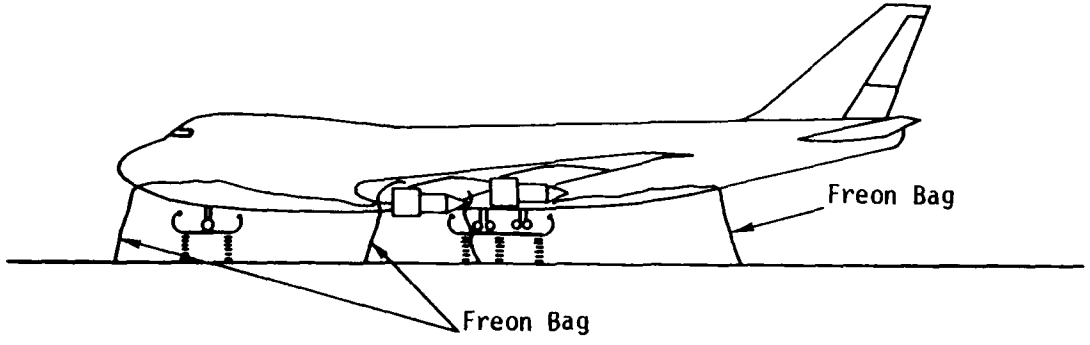

(b) Ramp/bridge assembly removed and top grading structure added, and Freon bags in place.

Figure 2. E-4B aircraft on dielectric isolation stand with Freon bags in place.

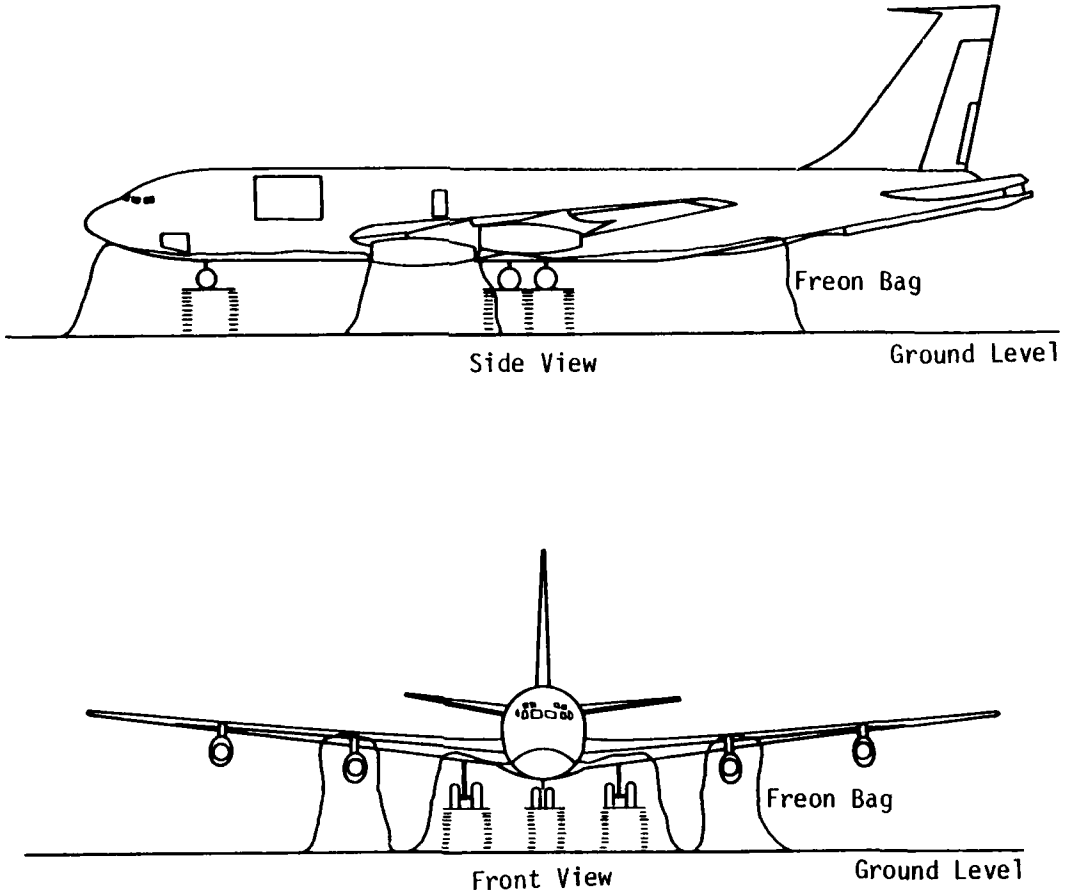

Figure 3. EC-135 aircraft on dielectric isolation stand with Freon bags in place.

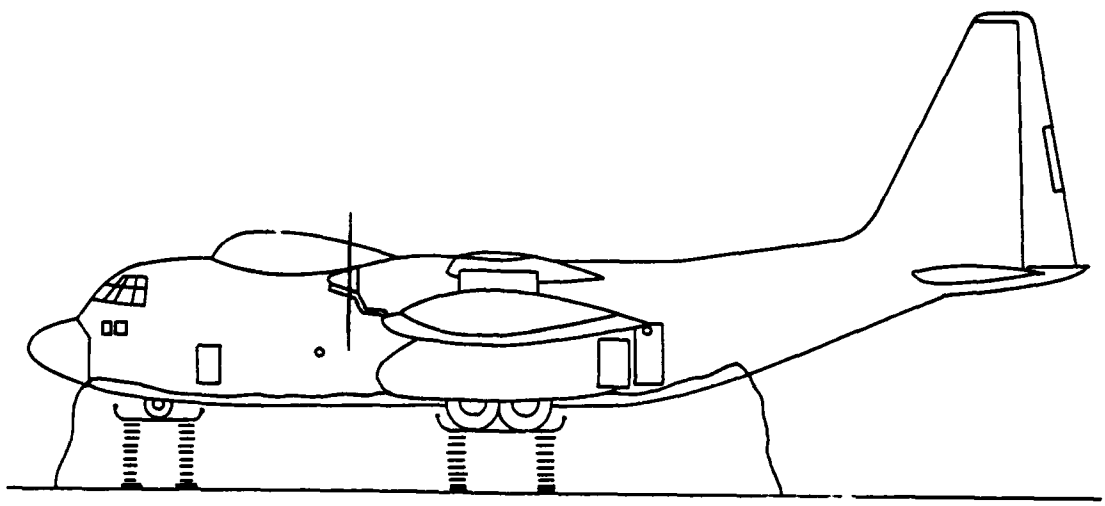

Figure 4. EC-130 aircraft on dielectric isolation stand with Freon bags in place.

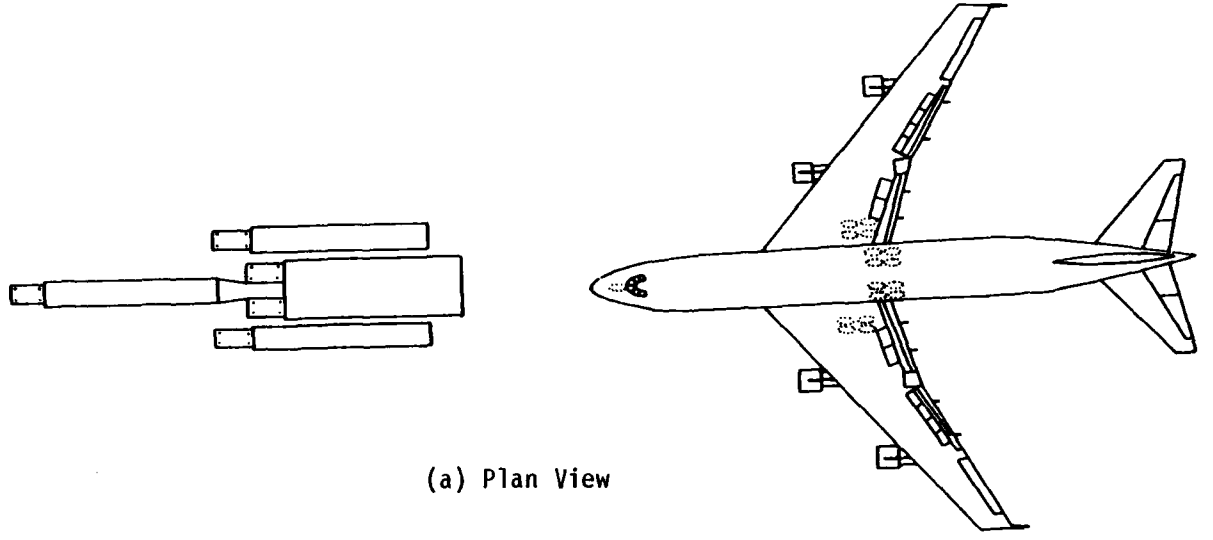

(a) Plan View

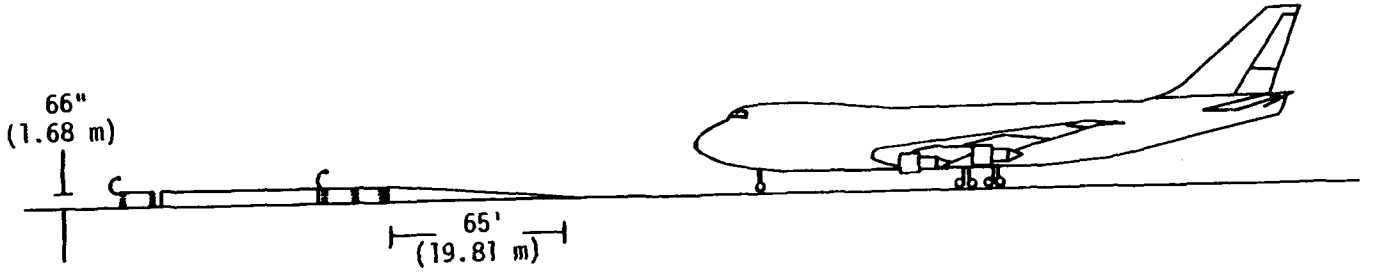

(b) Side View

Figure 5. Ramp/bridge assembly used to place the E-4B onto the isolation stand.

SECTION III
BASIC PHYSICS OF BREAKDOWN

The Townsend avalanche model is useful to explain the corona process; indeed, Ward (Ref. 1) has shown that the Townsend model is adequate to explain the entire breakdown transition in air near atmospheric pressure.

In the Townsend model, residual, free electrons, i.e., those caused by cosmic rays, photoionization, etc., are accelerated in the presence of an electric field. These accelerated electrons produce additional electrons, upon collision with gas molecules. When the magnitude of the electric field is sufficiently high, the colliding electrons, in the process of ionizing the air, produce an increase in electrons, so that the free electron density increases.

When such a condition occurs, so-called streamers start to form, and initiation of breakdown occurs. If the electric field remains high for a sufficiently long time, the streamer propagates from one electrode to the other, and breakdown takes place.

The parameter which measures the rate of increase of free electrons per unit volume is called the avalanche coefficient, and is a strong function of electric field strength. The major competing process to the production of electrons by ionization is the loss of electrons due to attachment, which in air is primarily oxygen attachment. The loss of electrons due to attachment, measured by a parameter called the attachment rate, is also a strong function of the electric field.

The avalanching and attachment of electrons can be summarized in the continuity equation for free electron charge, which is

$$\nabla \cdot \vec{i}_e + \frac{\partial \rho_e}{\partial t} = (G - \alpha)\, \rho_e + \dot{s} \quad ; \qquad (1)$$

where $\vec{i}_e$ is the electron current density,
ρ_e is the free electron charge/unit volume,
$G \equiv G(E)$ is the avalanche coefficient,
$\alpha \equiv \alpha(E)$ is the attachment rate,
$\dot{s}$ is the residual production rate of free electrons due to natural causes,
E is the electric field strength.

The quantities G and α have been empirically determined for air. Both of these parameters are functions of water vapor and pressure.

As the electric field is varied from low to high values, the quantity $G - \alpha$ changes sign. The character of the solution to Equation 1 simultaneously changes from a stable to an unstable condition. To determine the value of electric field at which instability initiates, empirical expressions for G and α were obtained from Reference 2, and are shown in Table 1. These values were used to numerically evaluate the solution of the nonlinear equation

$$G(E) - \alpha(E) = 0.$$

TABLE 1. EMPIRICAL EXPRESSIONS FOR ELECTRON ATTACHMENT RATE AND AVALANCHE COEFFICIENT IN MOIST AIR

Attachment Rate: $\alpha = (1-W)\,[(1+34.4W)\,\alpha_{3a} + \alpha_{2a}]\ (\text{sec})^{-1}$;

where $\alpha_{2a} = 1.22 \times 10^{8}\ \rho_r e^{-21.15/\varepsilon_o}$

$$\alpha_{3a} = 10^{8}\rho_r^{2}\left[\frac{0.62 + 800\varepsilon_o^{2}}{1+10^{3}\varepsilon_o^{2}[\varepsilon_o(1+0.03\varepsilon_o^{2})]^{1/3}}\right] ,$$

ρ_r is the relative pressure,

W is the fraction of the molecules which are H_2O.

Avalanche Coefficient: $G = \dfrac{5.7\times10^{8}\rho_r Y^{5}}{1+0.3Y^{2.5}}$;

where $Y = 10^{-2}\ \varepsilon_o$.

In the above expressions:

$$\varepsilon_o = \varepsilon/(1 + Ak);\ \varepsilon \doteq \varepsilon_1$$

$$= \left[\sqrt{\left(\frac{Bk}{2}\right)^{2} + \varepsilon} - \frac{Bk}{2}\right]^{2};\ \varepsilon_1 \doteq \varepsilon \doteq \varepsilon_2$$

$$= \varepsilon - Ck;\ \varepsilon \doteq \varepsilon_2 ;$$

where $k = p^{0.834}$,

$A = 2.457$,

$B = 0.6884$,

$C = 1.195$,

$\varepsilon_1 = 0.07853(a+Ak)$,

$\varepsilon_2 = 3.015 + Ck$,

$\varepsilon = E/p$ (esu/atmosphere),

E is the electric field in esu.

The curves shown in Figure 6 illustrate the results of this solution. As can be seen from Figure 6, air with a low moisture content becomes unstable for fields in excess of 1.74×10^6 volts/meter, at an altitude of 1.7 km (approximate altitude of Albuquerque).

Another equation, similar to Equation 1, can be written for ions. However, since the electrons are much lighter, their motion is predominant for short time scales.

In order to obtain some idea of the geometry required for corona initiation at Albuquerque altitude, consider the electric field surrounding an isolated sphere of radius r_o. The electric field is easily found through solution of Laplace's equation (5) and is

$$E(r) = -\frac{V_o r_o}{r^2} \text{ volts/meter}$$

where: V_o is the potential of the sphere in volts,

r_o is the radius of the sphere in meters,

r is distance from the center of the sphere in meters.

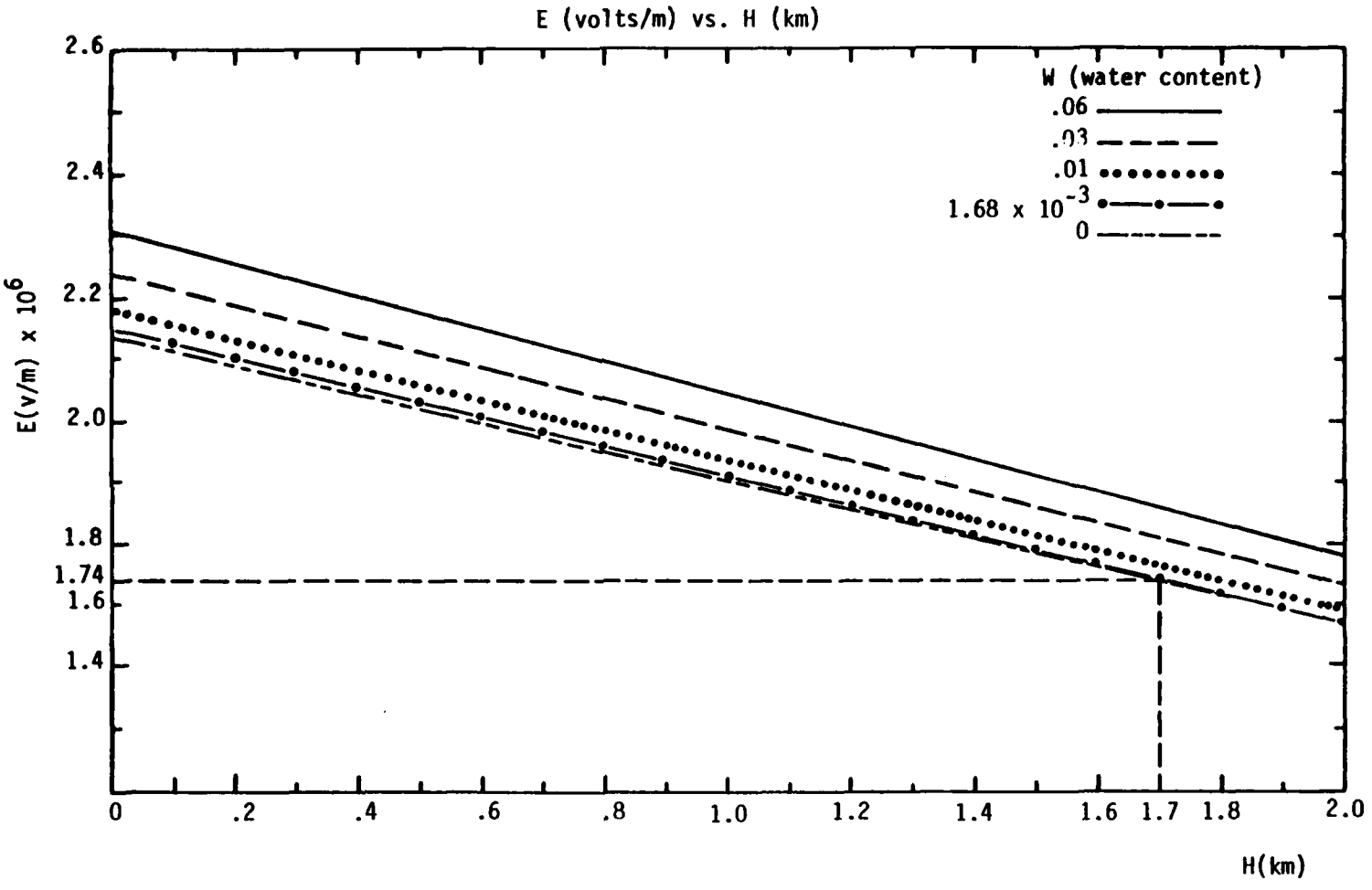

Figure 6. Threshold for unstable electron avalanching in air versus altitude and water content.

The highest field point occurs when $r = r_0$. For $V_0 = 3 \times 10^6$ volts, and at Albuquerque altitude, corona initiates at field strengths of about 1.74×10^6 volts/meter for dry air (see Figure 6). Consequently, corona will initiate for any sphere with radius less than 1.72 meters. As a result, it is difficult, if not impossible, to prevent corona from initiating from many points of the aircraft. Again, it is not intended to prevent corona, but only to prevent the aircraft from arcing to ground.

Of course, initiation of corona does not imply that breakdown will occur. In the case of the sphere, for example, corona may effectively increase the radius of the sphere until a point is reached where fields are below values required for instability.

Alternately, and more probably if the field is sufficiently high, streamers will start to form. In this case, breakdown will occur, if the streamer has sufficient time to propagate across the electrodes (in the present instance from the aircraft to ground).

The boundary conditions at the electrode surfaces, and the material of the electrodes, also influence the formation of streamers. If electrons are swept away from the electrode surface, additional electrons must leave the surface, if conduction current is to flow. In leaving the surface, these electrons must overcome the work function; therefore, the material in the surface, the surface condition (roughness), and the polarity of the applied voltage influence the breakdown potential.

Finally, we point out that gases, other than air, have differing electron attachment rates and avalanche coeffients. Therefore, corona initiation occurs at different electric field strengths.

SECTION IV
STREAMER ANALYSIS

As we have seen, when the electric fields are sufficiently high, streamers will form and breakdown will occur, if the streamer has sufficient time to propagate from one electrode to the other. Since corona will initiate at many points of the aircraft, streamer propagation times will determine whether or not the aircraft breaks down to ground. As a result, streamer analysis is a fundamental design tool in the sequel.

A cursory review of the pertinent literature indicates that information on breakdown is voluminous (see, for example, References 3, 4, and 5-17). References 3 and 4 probably contain the most complete discussion of streamer propagation.

The discussions in this section are intended to acquaint those readers unfamiliar with streamer analysis to the fundamentals of this art. Propagation of streamers, as discussed by Martin (Ref. 3), and Crewson (Ref. 4), form the basis of the following material.

The starting point for streamer analysis lies in the empirical relationship for a rising voltage applied across a gas-insulated, point-plane gap.

$$V_o^P \; T_o^Q \; d^M = \text{constant}; \qquad (2)$$

where: V_o is the breakdown voltage,

T_o is the time to breakdown,

d is the gap spacing,

P, Q and M are fixed exponents.

Equation 2 can be expected to apply not only to point-plane gaps, but also to gaps where the electric field is very divergent. This is the case for the potential breakdown points on the underside of the aircraft.

Martin (Ref. 3) has empirically determined the exponents in Equation 2, and states the result as

$$\frac{V_o}{d} \; T_o^{1/6} \; d^{1/6} = K \, p^n \quad ; \tag{3}$$

where: $\frac{V_o}{d}$ is the mean gap voltage,

p is the pressure in atmospheres,

K is a constant which depends upon the gas.

In the present case, the applied voltage is a 1/50 double exponential waveform (not a rising voltage), so that to proceed with this waveform, we must deduce a streamer-velocity relationship from Equation 3. Such a deduction is equivalent to finding a differential equation which has Equation 3 as solution. One might expect that there are many differential equations for which Equation 3 is the solution, and indeed, this is the case. The best one can do is to select a reasonable, streamer-velocity relationship, and verify the deductions from this relationship by experiment.

The relationship chosen by Crewson (Ref. 4) is

$$\frac{dx}{dt} = \frac{1}{5} \; \frac{V^6(t)}{(Kp^n)^{6x4}} \quad ; \tag{4}$$

where: $\frac{dx}{dt}$ is the streamer velocity,

x is distance along the streamer path,

V(t) is the applied voltage.

Martin (Ref. 3) gives the values of K and n listed in Table 2. These values are valid in the range of 1 to 5 atmospheres.

TABLE 2. VALUES OF K AND n FOR USE IN EQUATION 4

	Air	Freon	SF_6
K^+	22	36	44
K^-	22	60	72
n	0.6	0.4	0.4

The values K^+ and K^- refer to positive and negative voltages applied to the point electrode, respectively.

Following Crewson, we assume that the risetime of the applied pulse is much less than the fall time, so that most of the streamer's path is transversed on the falling portion of the pulse. Thus, the applied voltage is approximately

$$V(t) = V_o \exp(-t/\tau). \tag{5}$$

For purposes here, the time constant τ is equal to 50 microseconds.

Integrating Equation 5 from x = 0 to x = d, corresponding to t = 0 to $t = T_o$, results in

$$\left(\frac{V_o}{d}\right)\left\{\frac{\tau}{6}\left[1 - \exp(-6T_o/\tau)\right]\right\}^{1/6} d^{1/6} = Kp^n \tag{6}$$

We wish to determine the gap width, d, necessary to prevent flashover. This condition corresponds to a flashover time T_o of infinity. Therefore, Equation 6 yields the relationship

$$\left(\frac{V_o}{d}\right)\left(\frac{\tau}{6}\right)^{1/6} d^{1/6} = Kp^n \qquad (7)$$

Figure 7 is a plot of electrode spacing necessary to prevent flashover as a function of mean electric field (V_o/d). As can be seen from the data in this illustration, the aircraft will flashover unless significant precautions are taken.

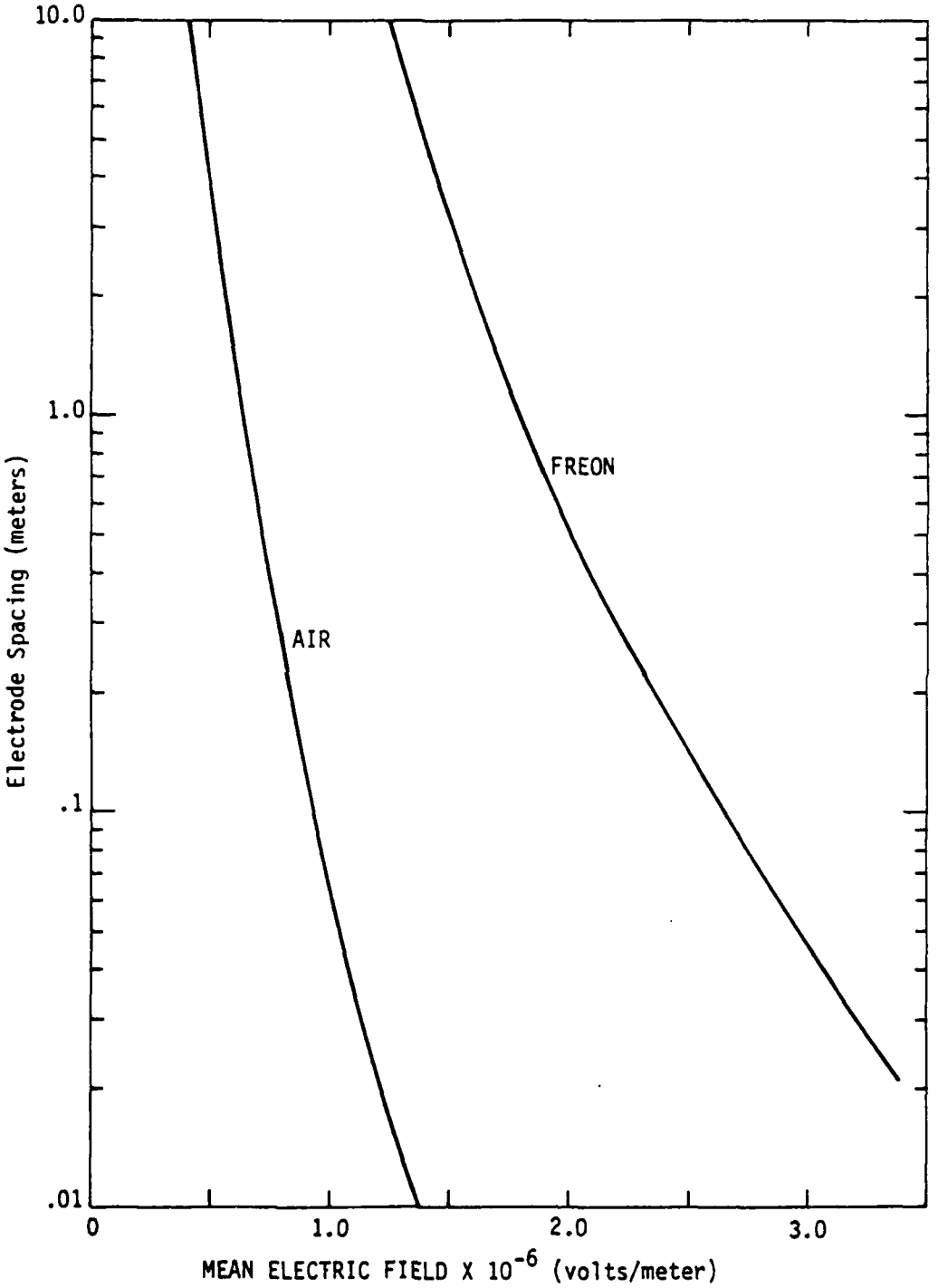

Figure 7. Electrode spacing necessary to prevent flashover for a divergent field.

SECTION V
AIRCRAFT ISOLATION ANALYSIS

INTRODUCTION

This section discusses the results of a study by Physics International Company (PI) to develop methods for electrically isolating aircraft during ground-based EMP tests. The effort was limited to an initial analysis of three types of aircraft. An analysis of the most probable points for high voltage breakdown from the aircraft to ground is developed. Methods of supporting and isolating the aircraft are proposed. An engineering concept of the support structure is presented. The dielectric materials to be used in the proposed solutions are discussed.

In order to simulate the electromagnetic pulse (EMP) of a nuclear detonation, high energy voltages and currents are introduced directly onto aircraft parked on the ground. Test results are significantly distorted by high voltage arcing between the aircraft and ground. The objective of this study was to develop methods of preventing this arcing during the tests. The principal areas of concern with regard to breakdown are the landing gear assemblies and lower portions of the fuselage, wings, and other appendages.

Three types of aircraft were presented for analysis: the E-4B, EC-130, and EC-135. The E-4B is the largest and heaviest, has the most complex wheel assemblies, and has protrusions from the undersurface of the fuselage similar to those on the other aircraft. The techniques and many of the hardware concepts for this aircraft would be directly applicable to the EC-130 and the EC-135. Thus the E-4B is the principal model used in this report.

The specified waveform of the electrical-transient input to the aircraft is a double exponential impulse with a 10 percent to 90 percent risetime of 1 μs and an e-fold falltime of 50 μs. The peak amplitude of voltage would be 3 MV. The electrical connection will be made by a wire connection between the aircraft tail and the high-energy, high-voltage impulse generator.

The recommended means of isolation consist of: (1) short dielectric columns on pads to support the aircraft; (2) gas-filled envelopes to raise the breakdown level surrounding these structures; and (3) similar envelopes or excavations around other parts, such as engine nacelles and tail protrusions.

Structural concepts are presented that allow for loading due to winds up to 80 knots. Large safety factors in supporting the static and rolling loads are considered. Portability is achieved through modularity.

A variety of dielectric materials are available for the support structures. The specific materials to be used would be chosen during a detailed design, cost, and availability study.

Other methods of accomplishing the required electrical isolation were considered and rejected. The reason for rejection of these methods involves lack of fidelity in the simulation achieved or the fact that the methods appeared to endanger the aircraft because of support stability problems. These methods will be discussed only briefly.

HIGH VOLTAGE ELECTRICAL ISOLATION ANALYSIS

Enhanced Electric Field Flashover

On all the aircraft studied in this program, there are relatively sharp projections, such as antennae or tail skid, extending away from the main body of the aircraft structures. When voltage is applied to the main aircraft structure, the maximum electric field that appears at the projection may be approximated simply by V/R, where V is applied voltage and is the minimum local radius of the projection. For instance, if an antenna has a minimum radius of about 0.5 cm (typical of the antenna projections on the E-4B), the local electric field with 3 MV applied is approximately 6 MV/cm. The breakdown strength of atmospheric air (at sea level) is approximately 30 kV/cm. Therefore, the air in the vicinity of the antenna will break down, and an electric streamer will extend toward the ground plane in the general direction of the local electric field. Indeed, this effect is desired, since it occurs on an aircraft in flight. However, flashover will take place if the streamer reaches the ground plane while substantial voltage persists on the aircraft structure. Therefore, the flashover to ground of the aircraft structure (at the point of the sharp projection) depends on the amplitude and pulse shape of the voltage applied to the aircraft.

For highly divergent electric fields such as those just described and for gaps greater than 10 cm, J. C. Martin of AWRE has developed the following relationship:

$$F_{\pm} (dt)^{1/6} = K_{\pm} p^{n}$$

where F is the maximum mean electric field at breakdown (V/d) in kV/cm, d is the gap length in centimeters, t is the 88 percent amplitude pulse width in microseconds, and p is in atmospheres (see "Circuit and Electromagnetic System Design Notes," Note 4, Nanosecond Pulse Techniques by J. C. Martin, AWRE, April 1970, p. 14). Martin's values for K and n are given in Table 2.

Flashover is also dependent on the polarity of the voltage pulse on the highly enhanced projection as indicated by the $\pm$ polarity indicators.

Martin's relationship describes the conditions present when flashover occurs. W. C. Crewson of Pulsar Associates, Inc., redefined Martin's relationship for highly enhanced electric fields when one wished to avoid flashover ("Switching Notes," Note 11, Operating Theory of Point-Plane Spark Gaps by Walter F. Crewson, March 1971). For exponentially falling waveforms as are involved in this study (one microsecond risetime to 50 microsecond falltime), Crewson's relationship to avoid flashover may be written as

$$F_{\pm} \left(\frac{\tau}{6}\right)^{1/6} d^{1/6} = K_{\pm} p^{n}$$

where the quantities are as previously defined except that τ is the e-fold of the exponential falltime.

Using this relationship, one can determine the conditions to just avoid flashover for highly enhanced electric fields situations.

To test the validity of this theory, two cases of previously built high voltage generators were examined: SIEGE II and VPD II.

The SIEGE II output pulse has a 50 microsecond exponential decay. The SIEGE II output line had a 3 meter spacing, and the peak amplitude of the voltage was 2 MV. The SIEGE II model line was tested in Albuquerque ($\sim$ 5000 feet altitude, p = 0.8).

Therefore,

$$F \left(\frac{\tau}{6}\right)^{1/6} d^{1/6} = 22\ p^{n}$$

to just avoid flashover

$$(6.66)\ \frac{kV}{cm} \left(\frac{50}{6}\right)^{1/6} (300)^{1/6} \stackrel{?}{=} 22\ (0.8)^{0.6}$$

$$\sim 25 \neq \sim 15$$

If the quantity on the left is larger than the quantity on the right, one would expect flashover. In general, the SIEGE II model antenna did not flash over indicating some safety factor in our computation. However, night photographs of the antenna showed a myriad of streamers--especially from the partially graded edges of the line--that appeared to bridge the gap to the ground. These photos indicated that the line was very near to flashover at the Albuquerque altitude and are considered to be a confirmation of the analysis method.

VPD II (also located in Albuquerque), has housing that is known to flash over at about 4 MV. This housing is immersed in Freon at about atmospheric pressure. The housing length is approximately 160 cm in height and sustains an exponential decay of about 0.282 microseconds e-fold at 4 MV. Applying the analysis:

$$\left(\frac{4000}{160}\right)\left(\frac{0.282}{6}\right)^{1/6}(160)^{1/6} \stackrel{?}{\leq} (60)(0.8)^{0.4} \quad \text{or} \quad (36)(0.8)^{0.4}$$

$$35 \neq 55 \text{ for negative enhancement}$$
$$\text{or}$$
$$33 \text{ for positive enhancement}$$

The analysis indicates that the VPD II output switch housing should be safe for negative enhancements and should just flash over for positive enhancements. A grading shield around the base of the switch housing does provide positive enhancements; this case is also considered to be a confirmation of the analysis method.

One should remember that in both the SIEGE II AND VPD II example given, large-radius grading structures were added to avoid or delay streamer formation, but that streamers did occur. Both systems are operated near their maximum field limits at 2 MV for SIEGE II and 4 MV for VPD II.

Therefore, assuming the validity of this analysis, which is based on the streamer transit time across an enhanced gap, the design of the aircraft EMP isolation reduces to determining the minimum distance from an enhanced point on an aircraft to ground that will flashover. Rearranging the W. C. Crewson equation to solve for the distance (realizing that F = V/d) gives

$$d_{\pm} = \left[\frac{V_{\pm}\left(\frac{\tau}{6}\right)^{1/6}}{K_{\pm}\, p^{n}}\right]^{6/5}$$

This equation was solved for $V_{\pm}$ = ± 3000 kV, τ = 50 microseconds, and for altitudes of 0 and 1.52 km. The results are shown in Table 3.

TABLE 3

FLASHOVER DISTANCE FOR ENHANCED GAPS (feet)

Altitude (km)	Air	Air (SIEGE Data)	Freon Negative	Freon Positive	SF_6 Negative	SF_6 Positive
0	18	13	5.5	10	4.4	7.9
1.52	20	15	6	11.25	4.9	8.8

Table 3 shows that in air at an altitude of 1.52 km, sharp projections on the aircraft must be 6.1 m from the ground to avoid flashover or 5.49 m at sea level. The second column is derived from the fact that the SIEGE II array should have flashed over but it did not. This implies a value of 29 for the constant K for air and 50 microsecond e-fold pulses. In this report, the second column (SEIGE data) was used for the design of the aircraft isolation. If a point on the aircraft is less than 4.57 m from the ground plane (for an altitude of 1.52 km), that point must be immersed in Freon or SF_6. The designs presented here assume that Freon is the gas used and that the polarity of the output pulse is negative.

Higher stresses than those implied by the distances in Table 3 may be used if the electric field in the gap is kept strictly uniform. Therefore, to avoid high dielectric stands, a uniform field stand is designed for the wheel supports to maximize the allowable electric field strength and therefore minimize the flashover distance. The stand is designed to be immersed in Freon at the local atmospheric pressure.

Uniform Field Flashover Analysis

J. C. Martin gives the following expression for uniform field breakdown in air (Circuit and Electromagnetic System Design Notes, Note 4, p. 12, previously cited):

$$E = 24.6\ p + 6.7\ p^{1/2}/d^{1/2}\ \text{kV/cm}$$

where p is the atmospheres and d is in centimeters. For gaps of approximately 1 meter, this implies 25.27 kV/cm at sea level in air and 20.28 kV/cm at 1.52 km. The usual improvement in the dielectric strength realized by using Freon is 2.5 times that for air under the same conditions. (SF_6 has about 2.7 times the dielectric strength of air.) However, as mentioned by J. C. Martin in the note cited, there are nonlinearity effects for the hard gases. These nonlinear effects are dependent on the gas pressure and the gap length. PI experience would indicate that with the gap length cited ($\sim$ 1 meter) and using negative polarity, approximately a factor of 2.0 can be realized by using Freon instead of air. Therefore, the breakdown strength to be used is 40 kV/cm at an altitude of 1.52 km. This implies that a stand height of 75 cm would break down just at 3.0 MV (negative polarity). However, since the ultimate hold-off is along a dielectric surface (the support stand), an even further relaxation of the stress is required. The stand must be uniformly graded to avoid field nonuniformities; that is, the subject of the following discussion.

The Techniques of Isolation

In order to sustain 3.0 MV impulses on the aircraft under test, these aircraft must be suitably supported from ground, and all structural areas liable to high electric field enhancements must be modified to reduce the enhancement or be surrounded by a gas which is electrically superior to air.

The method of support is of most concern, for this is required to be simple and to yield structures which are mechanically safe and transportable.

Although not exclusive, the solid dielectric platform arrangements are appropriate to this duty, and the size of these platforms depends upon the efficiency of solid dielectric use.

In this report, we present two dielectric platform arrangements which use common techniques of solid dielectric usage, but which differ in matters of volume, modularity, and manufacturing control.

Solid Dielectric Insulator Efficiency

The intrinsic electrical strengths of solid dielectrics are high. For materials such as Lucite and epoxies, the volume breakdown strengths are in the range 5 to 10 MV/cm. Such electrical strengths can rarely be exploited in equipment design, since the flashover strengths of the solid dielectric surfaces in contact with gaseous or liquid media are one or two orders of magnitude lower. Such is the case for the aircraft support problem, where the ultimate dielectric strength of a platform structure is dependent upon the solid-gas interface along its height. The best that can be done, in a gross sense, is to arrange for the electric field to be uniform along the height of the dielectric support structure. In dielectric terminology, uniform voltage grading of the dielectric support is required.

For impulsive voltages, the voltage grading of an insulator is determined by the inherent capacities, and for steady-state voltages, the grading is determined by the dissipative elements, such as surface resistance.

The capacities must then be ordered to give the desired impulse grading, and the discharge currents must be made substantially uniform along the height of the insulator.

If the insulator height is subdivided at equal intervals by metal planes, then the insulator is a structure of equal capacities in series; in the absence of significant stray capacities to ground, compulsive voltages will distribute uniformly along its length.

The deleterious effect of stray capacities to ground, for the special case that these capacities are equal from each tier of the structure, is shown in Figure 8.

The effect of stray capacities to ground may be reduced to acceptable levels by increasing the segmentation of the insulator to increase the capacitance per unit length or, if this has reached a practical limit, by balancing the displacement currents to ground and the high voltage terminal at any point, as illustrate in Figure 9.

Outstanding applications of this graded insulator technology are to be seen in the insulated column structures of modern Van de Graaff accelerators. These columns are plane assemblies of glass or ceramic bonded to metal; they have high electrical efficiency and mechanical strength. Figure 10 illustrates a typical modular assembly with the major mechanical loadings.

When it has been arranged that the electric fields are uniform along the dielectric structure of the support platform, attention must be given to the electrical efficiency of each segment of the dielectric structure.

The major influence on insultator efficiency, i.e., the ratio of electric insulator, is the condition of the metal electrode and solid dielectric interface, particularly where this interface meets the gas (the "triple point"). Figure 11 emphasizes the imperfections that can occur, and Figure 12 shows the lowering of insulator efficiency that results.

If care is taken with these metal-dielectric interfaces, the insulator efficiencies can be high, as shown in Table 4. In practice, these efficiencies will be reduced to the range 0.1-0.7 by the inevitable imperfections in large structures, and by surface contaminations to be expected in the field environment.

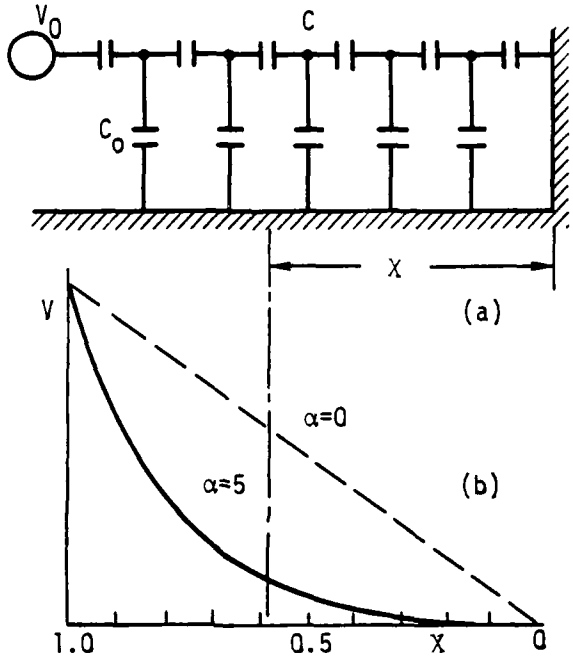

$$V_X = V_0 \ (\sinh \alpha x / \sinh \alpha)$$

where

$$\alpha = \sqrt{(C_0/C)}$$

Figure 8. The transient voltage grading problem.

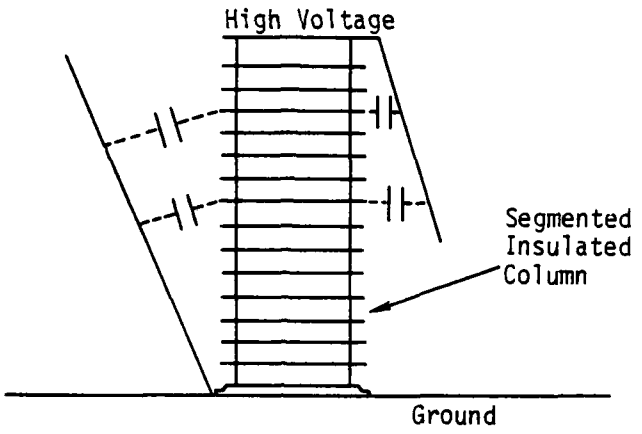

Figure 9. Improved voltage grading by balanced displacement currents.

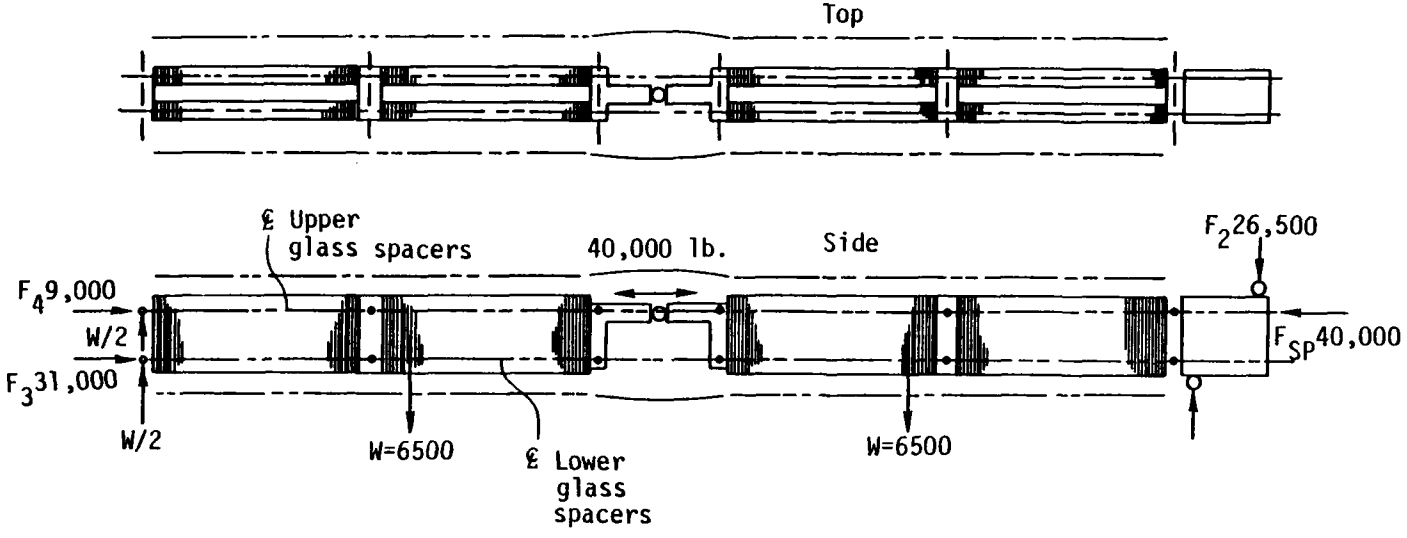

79-6-171

Figure 10. Schematic longitudinal section of H.V.E.C. horizontal tandem.

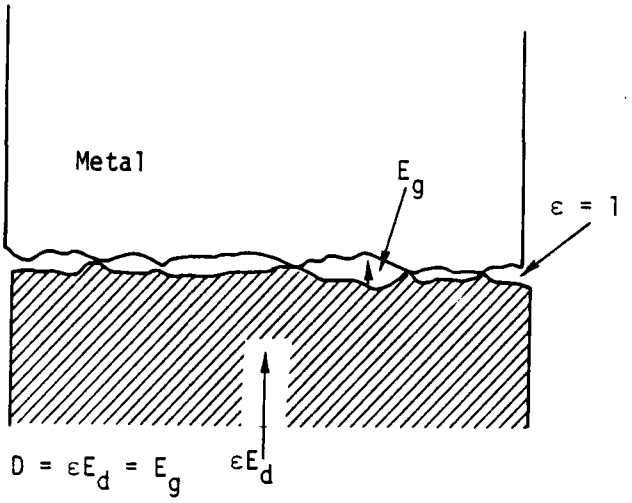

Figure 11. Representation of dielectric/metal interface.

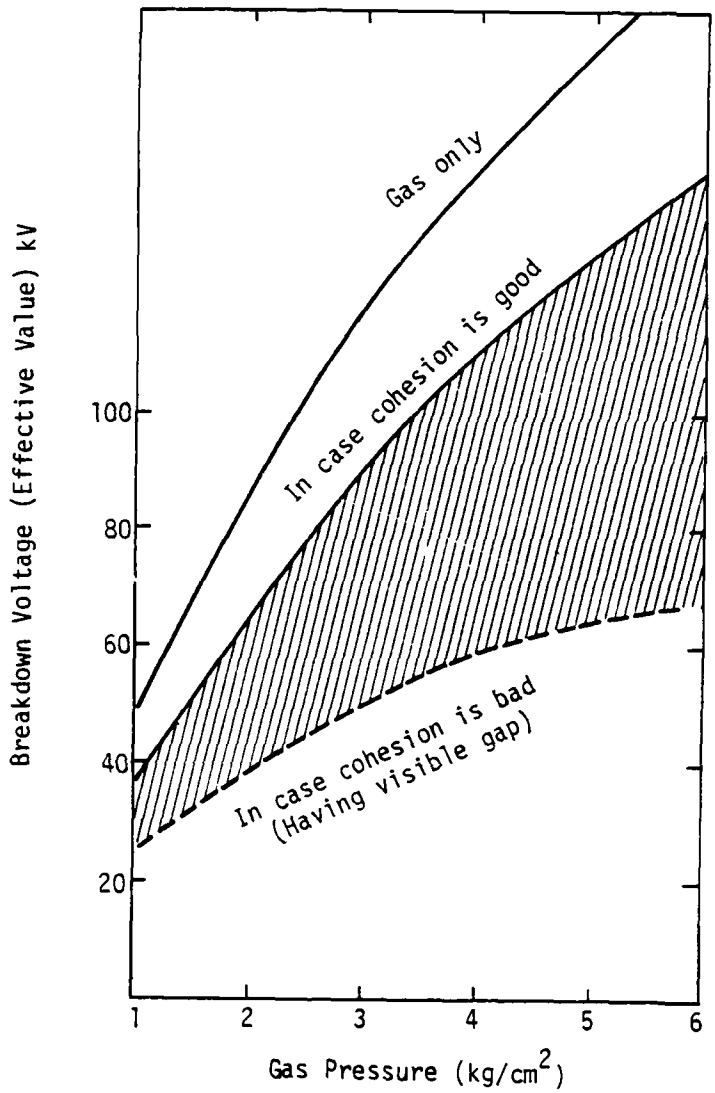

Figure 12. Effect of cohesion in case of coaxial electrode.

Table 4

Mean spacer efficiencies for the flashover of cylindrical insulators in a uniform field in SF_6
(1 or 2 cm long spacers; temperature--20° C)

APPLIED VOLTAGE	dc			ac			Impulse			ε^+
Pressure psia	15	30	45	15	30	45	15	30	45	--
Polymethylemethacrylate	.93	.86	.65	.90	.84	.68	1.0	.94	--	3.5
Polypropylene	.91	.88	.75	.94	.94	.93	.93	1.0	.89	2.2
Polytetrafluoroethylene	.86	.87	.81	.92	.88	.86	1.0	.92	--	2.1
Nylon II	.77	--	--	.95	.79	--	.97	.97	--	3.7
Epoxy Resin	.95	--	--	.89	--	.78	--	--	--	4.5
Glass/Eposy Laminate	.91	.79	.71	.74	.62	.54	.93	.84	.76	4.8
Glass	.87	.74	--	.77	.72	.60	--	--	--	5.0
Glazed Porcelain	.84	.76	--	--	--	--	--	--	--	6.5
Unglazed Porcelain	.71	.57	.51	.78	.63	.52	--	--	--	6.5
SRBP* Rod	.47	.34	.25	.72	.60	.51	.91	.85	.79	3.8
SRBP* Tube	.45	.31	.23	.61	.48	.44	.87	.67	.59	3.8
Synthetic Resin Densified Wood	.37	--	--	--	--	--	--	--	--	--

*Synthetic resin bonded paper.

†Typical values--may be frequency dependent--care should be taken in using these numbers--generally similar materials (e.g., epoxies) can have quite different values.

With uniform field grading and the assumption of a 0.6 insulator efficiency, the minimum length of dielectric surface for a 3.0 MV impulse at S.T.P. would be about be about 200 cm at an altitude of 1.52 km. In order to reduce the minimum to about 100 cm, the support structure must be immersed in a superior gas such as SF_6 or Freon 12. Using the factor of 2.0 for Freon as described earlier in this Section (Uniform Field Flashover Analysis), an insulator length of 100 cm is chosen.

Dielectric Support Protection

In the event of a surface dielectric breakdown along the support structures, surface "tracking" or dielectric destruction could occur. To avoid this, each section of assembly should be protected by an array of adjustable, but simple, spark gaps with suitable series, dissipative elements if possible.

The Aircraft Isolation Support Structure

The height of the stand will be larger than the chosen 1.0 m insulator length so that the metallic grading separators may be inserted and because some metallic members are required for the ends of the support stand to uniformly transfer the load of the aircraft to the dielectric support members.

One method of supporting the E-4B aircraft is illustrated in Figure 13. Acrylic sheets, 1.78 m by 3.05 m by 1.27 cm are uniformly laminated with aluminum grading spacers to make a stack approximately 1.27 m high. A 5.08 cm aluminum plate on each end of the stack makes a total height of 1.37 m. The top plate is required to help spread the wheel loading to a larger area of acrylic. The bottom plate is required for handling the stand as a modular unit--one such module for each of the four main landing gear assemblies and one for the nose gear assembly. Each of the main landing gear isolation stand modules (called flat-type module) weighs approximately 15,422 kg.

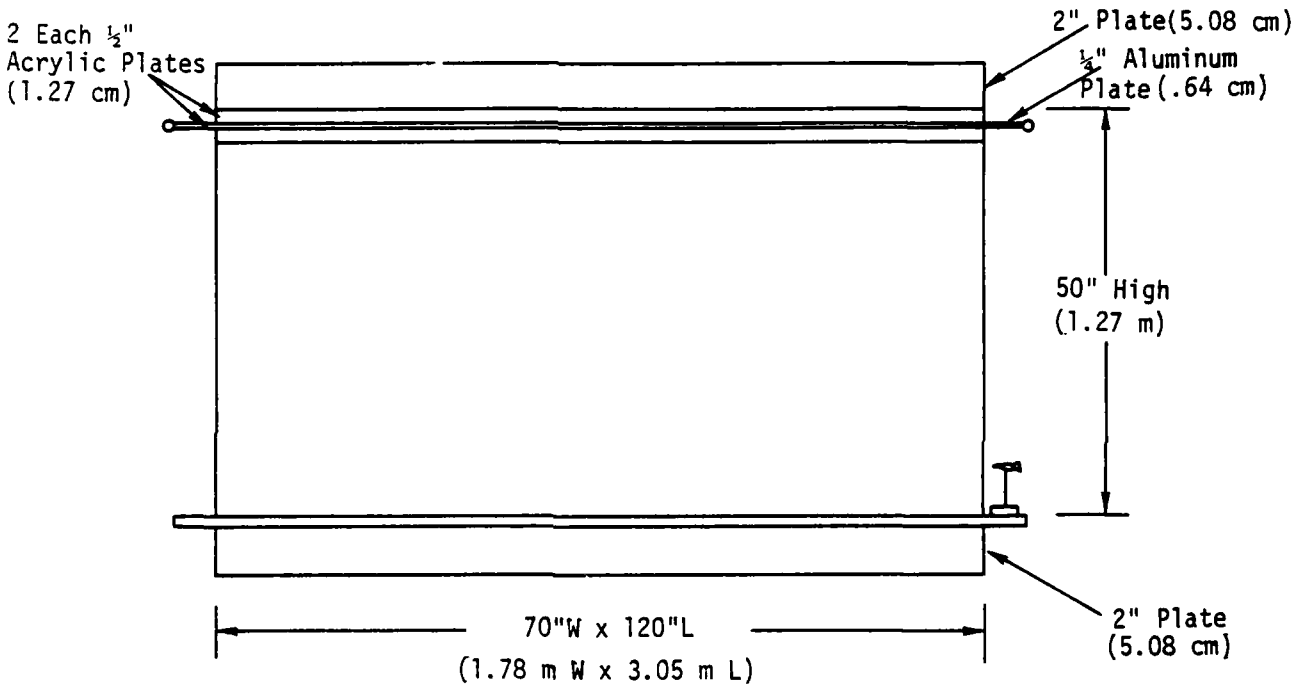

Figure 13. A version of an insulator support stand for the E-4B aircraft.

Acrylic sheet is available in the size described, and even slightly larger sheets are available in the 1.27 cm thickness.

The edges of the interleaved aluminum grading plates are radiused to minimize sharp edges. Alternate plates extend beyond the edge of the acrylic and have a circular cross-section "bead" around the edge. These "beaded" edges act as grading rings and also will act as spark gaps should the stand flashover. Sparking will therefore take place away from the plastic interface surface and avoid damage to the stand should a flashover occur. This feature is illustrated in Figure 1.

Figure 1 shows the laminated sheet type of stand (flat-type stand) supporting a main landing gear of the E-4B aircraft. Also illustrated in Figure 14 is a top grading structure used to isolate and protect the vicinity of the landing gear. The landing gear doors are also shown protected, but the top grading terminal could be made less complex if these doors could be removed.

Figure 14 shows another type of stand for support of the E-4B aircraft. This stand is called the "column-type isolation stand" because it is supported by four columns. The insulator columns for this type of stand have the same basic laminated structure as for the flat-type stand. Spark gaps will be arranged at the edge of the metallic grading laminations to avoid flashover along the insulator surface. The height of the aircraft in this type of isolation structure is 1.70 m because a structural platform capable of handling the landing gear assembly loading must be mounted on top of the columns. Details of the top grading structure to protect the tires and the wheel well doors is similar to the flat type of isolation support.

A more detailed sketch of the support column structure is shown in Figure 15. The column-type stand module weighs approximately 3600 kg.

Placing the aircraft onto either type of isolation structure requires a combination ramp/bridge assembly. The angle of the ramp must be limited to 5^{o} or less according to Boeing engineers. Therefore, the length of the ramp for the flat type structure is 15.7 m minimum. For the column type structure, the ramp length is 19.2 m.

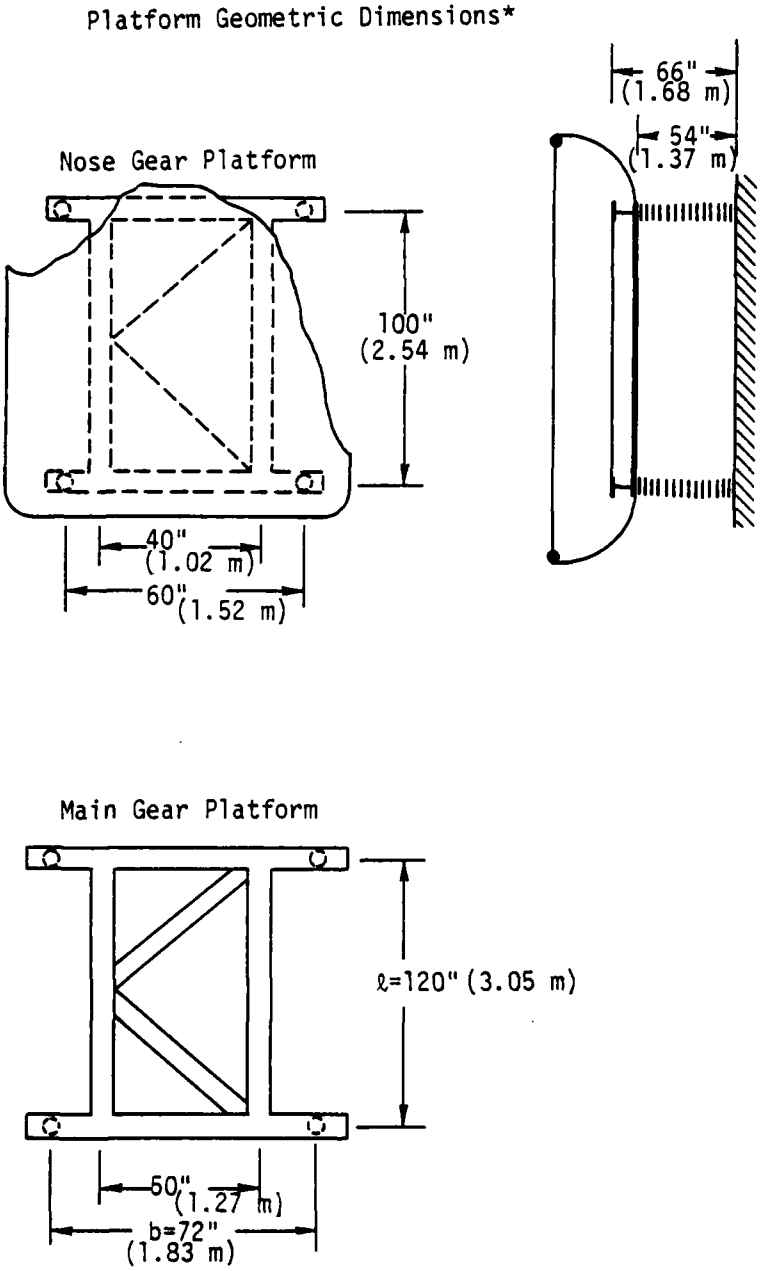

**Refer to Boeing 747, DG-14043, Section 3, pp. 45, 68.*

Figure 14. Column-type isolation stand for the E-4B.

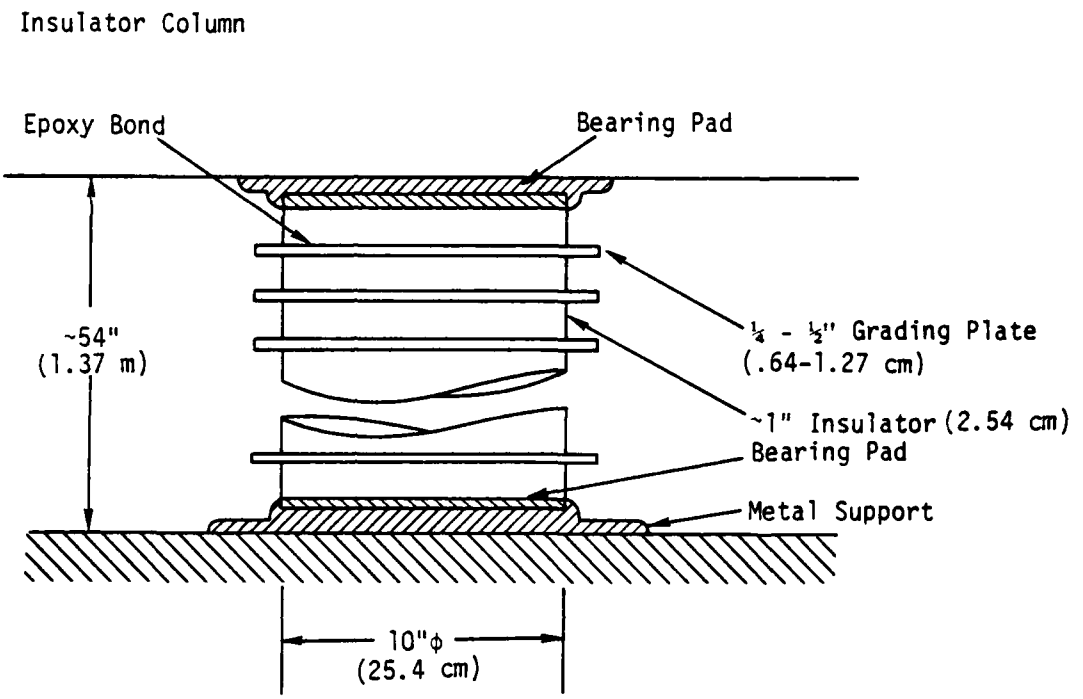

Figure 15. Details of the support column for the column-type isolation stand.

The ramp/bridge principle is illustrated in plane and side views in Figure 5 for the E4-B aircraft and the column-type structure. After the aircraft is rolled onto the support structure, the ramp/bridge assembly is removed and the top grading terminals are put in place. An illustration of the E-4B on the column-type isolation stand, before and after ramp/bridge assembly removal, is shown in Figure 16.

The EC-135 aircraft is shown on a dielectric support stand in Figure 5. The EC-130 is shown on a dielectric support stand in Figure 17.

Figure 3, 16b, and 17 also illustrate the approximate placement of the Freon bags used to immerse the dielectric stands and the aircraft undersides in Freon.

Using Table 3, one can easily determine whether Freon is required for any particular point on the aircraft. Freon must be used if any point on the aircraft is closer to the ground than 4.59 m as the aircraft is sitting on either type of stand (Table 3, Column 2, 1.52 km). In Freon, any place on the aircraft more than 1.84 m from the ground is safe from flashover. The dielectric stands, of course, must also be surrounded by Freon.

Physics International and MRC made measurements of the three subject aircraft, the E-4B, EC-135, and EC-130.

Measurements of the E-4B indicate that the entire underside of the aircarft's fuselage and the engine nacelles must be protected by Freon. The outboard engines could alternately be protected by scooping out the earth beneath the engines to a depth of 1.22 m or 1.53 m depending on the height that the isolation stand lifts the aircraft.

From the measurements made on the EC-135, it appears that the entire underside of the aircraft including the wings must be protected by Freon. Alternately, a higher stand could be built or a lower voltage used.

The EC-130 aircraft must also be Freon protected over its entire underside, including the wings.

The EC-130 also requires the 1.68 m height of the column (or a higher version of the flat-type stand) due to the extremely low ground clearance of

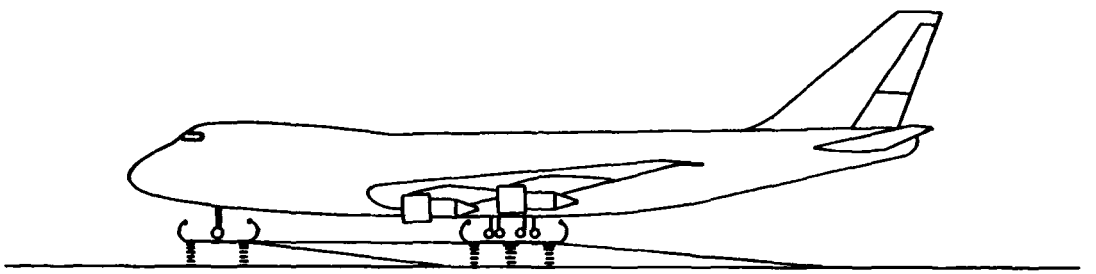

(a) Ramp/bridge assembly in place with top grading structure added.

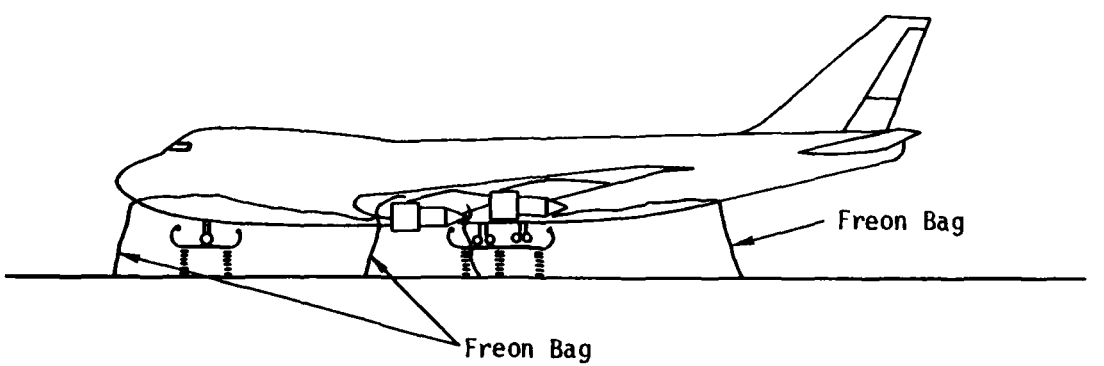

(b) Ramp/bridge assembly removed and top grading structure added, and Freon bags in place.

Figure 16. E-4B after placement on column-type structure.

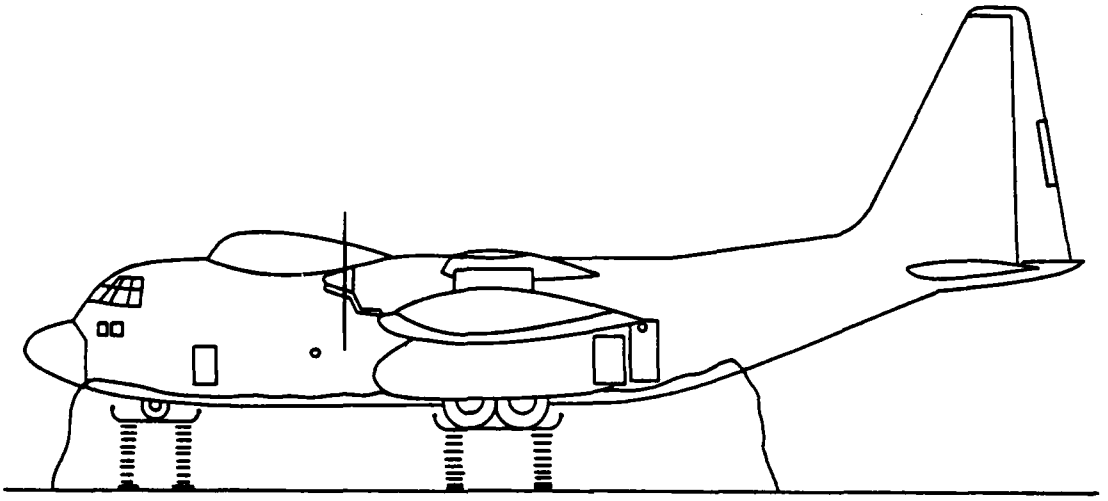

Figure 17. EC-130 is shown on dielectric isolation stand.

the fuselage. Even at the 1.68 m stand height, projections (such as the tank skid) on the underside of the EC-130 are close to the flashover threshold (the tail skid clears the ground by only 20.32 cm.

Higher stands could be built for the EC-130, or lower voltage could be used for the EC-130 tests to ease the Freon protection requirements.

The concept for the Freon bag construction is to use some heavy, but inexpensive, plastic sheet such as .05 cm thick polyethylene. The bag would consist of continuous floor and side walls and be taped to the aircraft with a commercially available dielectric tape.

The next section discusses the structural adequacy of the isolation stand designs and the insulator materials that were studied during the program. Liquid insulators were rejected early in the program as not being suitable for aircraft isolation since they are nonstructural, and a solid insulator/gas interface is required. Ultimately, it is desirable that a large part of the aircraft (especially the E-4B) must be insulated by the local natural atmosphere.

STRUCTURAL ANALYSIS AND MATERIALS

Introduction

Insulating platforms are needed to support the weights of the airplanes during EMP tests. Based on fabricating and handling considerations, it is advantageous to provide a separate platform for each landing gear assembly. The airplane is positioned on the platforms by towing it up a 5^{o} grade steel ramp/bridge structure (see Figure 18a).

Two types of insulating platforms are reviewed for their structural adequacy. The column type is a 1.78 m x 3.05 m steel-framed top platform with four 25.4 m diameter corner insulating support columns. The support columns consist of layered insulating discs bonded between thin aluminum gradient plates. The flat type is a 1.78 m x 3.05 m rectangular layer-graded platform. It is a solid composite structure of acrylic sheets bonded between thin aluminum plate. Construction details of these platforms are shown in Figures 1 and 14.

Loads

To analyze the structural adequacy of the platform, three loading conditions are considered:

1. Airplane gross weight plus platform structural dead weight
2. Axial load due to towing
3. Lateral load due to wind.

The breakaway resistance of an airplane is given as*

$$F_A = 0.04\,\overline{W}$$

where $\overline{W}$ = maximum gross airplane weight. This load could be resisted by the ramp. In this analysis, however, it was considered that the load will be resisted by the platform.

*Refer to Boeing 747, D6-14043, Section 5,(HIGH VOLTAGE ELECTRICAL ISOLATION ANALYSIS).

The wind pressure is given by

$$p = 0.003\ (V)^2$$

where

V = wind velocity in mph.

The lateral load on the platform due to wind can be computed as follows:

$$F_L = 0.67\ p\ A_L$$

where A_L is the lateral cross-sectional area of the airplane.

Consider the case of the Boeing 747-200 airplane and a column-type platform. The airplane's gross weight, $\overline{W}_s$, is 808,000 lb (see Table 5); the platform structural dead weight, $\overline{W}_s$ equals 6,000 lb, and the axial load due to towing, F_A is $0.04\ \overline{W}$ = 32,000 lb. In the wind of 80 knots, the wind pressure,

$$p = 0.003\ (1.15 \times 80)^2$$

$$= 25.4\ \text{lb/ft}^2.$$

The lateral cross-sectional area of the airplane

$$A_L\ 5520\ \text{ft}^2.*$$

Therefore, the lateral load due to wind for this case is:

$$F_L = C_W\ p\ A_L$$

$$= 0.67\ p\ A_L$$

$$= 94{,}050\ \text{lb}$$

Local wheel loadings are calculated as follows:

Nose gear wheel loading:

$$F_N = \quad = 46850\ \text{lb.}$$

Nose gear breakaway resistance:

$$F_{NA} = 0.04\ V_{NG} = 3748\ \text{lb.}$$

*Refer to Boeing 747, D224-10009-1.

V_{N_G} = Maximum vertical nose-gear ground load at most forward CG*

V_{M_G} = Maximum Vertical main-gear ground load at most aft CG

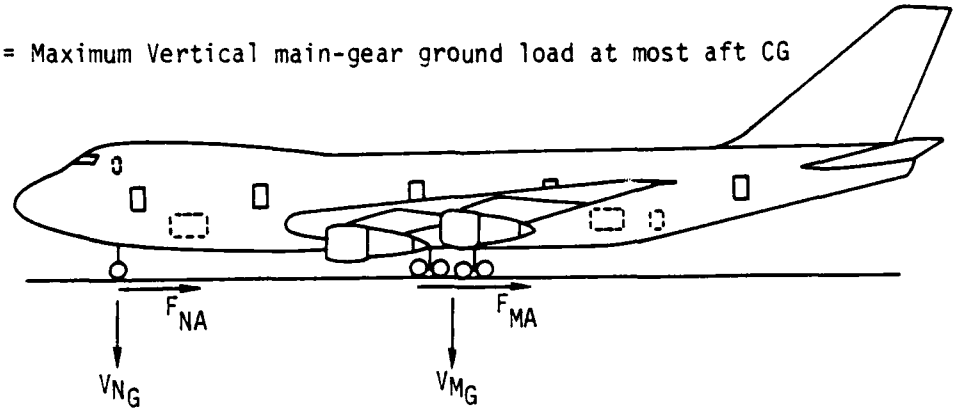

Table 5. Load characteristics of the Boeing 747.

Airplane	Maximum Gross Weight		V_{N_G}		V_{M_G} Per Strut (4)	
			Static at Most Forward CG**		Maximum Load Occuring at Static Aft CG	
	LB.	KG.	LB.	KG.	LB.	KG.
747-100	713,000	323,700	74,900	34,000	166,500	75,600
747-100	738,00	335,000	76,800	34,900	170,500	77,400
747SR	523,000	237,400	53,300	24,200	125,900	57,200
747SR	603,000	273,800	62,700	28,500	145,200	65,900
747SR	713,000	323,700	77,700	35,300	166,500	75,600
747SR	738,000	335,000	76,800	34,800	170,500	77,400
747-200	823,200	373,600	93,000	42,200	189,900	86,200
747-200	808,000	366,800	93,700	42,500	186,000	84,400
747-200	778,000	353,200	90,200	41,000	181,700	82,500

*Refer to Boeing 747, Db-14043, Section 3, p. 77b.

**All static loads calculated using airplane maximum gross weight.

Main gear wheel loading:

$$F_M = \frac{V_{MG}}{4} = 46{,}500 \text{ lb.}$$

Main gear axial breakaway resistance:

$$F_{MA} = 0.04\ V_{MG} = 7440 \text{ lb.}$$

Similarly, the loads for airplanes EC-130G and EC-135(K) can be obtained (see Table 6).

When these loads were compared, it was found that the platform designed for the Boeing 747-200 is also adequate for the EC-130 and the EC-135.

Design Criteria

Platform. AISC specifications on A-36 structural steel shall be followed. All components of the structure shall be proportioned so that the working stresses shall not exceed the following values:

Tension, $\sigma_t = 0.60\ \sigma_y$, σ_y = yield strength

Shear, $\sigma_s = 0.40\ \sigma_y$

Bending, $\sigma_b = 0.66\ \sigma_y$

Compression, $\sigma_c = \left[1 - \frac{(k\ell/r)^2}{2C^2}\right] \frac{\sigma_y}{S.F.}$

$$C = \sqrt{\frac{2\pi^2 E}{\sigma y}}$$

$$S.F. = \frac{5}{3} + \frac{3(k\ell/r)}{8C} - \frac{(k\ell/r)^2}{8C^3}$$

Weld allowable stress, σ_w = 13650 psi.

Beams and girders shall be proportioned so that the maximum live load deflection will not exceed 1/800 of the span.

Table 6. Load characteristics of the EC-130G and EC-135(K) aircraft.

Airplane	Maximum Gross Weight (lb)	Maximum Vertical Ground Loads (lb)		Axial Breakway Resistance (lb)	Laterial Wind Load @ 80 Knots (lb)
		Main-Gear	Nose Gear		
747-200	800,000	186,000	93,700	7,440	94,050
EC-130 G	175,000*	70,000	59,000	3,000	23,000
EC-135(k)	301,000	125,000	90,000	5,000	34,100

*155,000 lb is recommended, 175,000 lb is overload.

Platform structural dead weight:
Column type = 8000 lb
Flat type = 34000 lb

Insulator Columns. The insulator columns are graded nonmetallic structural components. To ensure their structural integrity, the working stresses shall not exceed the following values:

Tension, $\sigma_t = 0.20\ \sigma_{ult.t}$, $\sigma_{ult.}$ = ultimate strength

Compression, $\sigma_c = 0.20\ \sigma_{ult.c}$

Shear, $\sigma_s = 0.20\ \sigma_{ult.s}$

These limitations will cover environmental effects on the nonmetallic part of the column.

Some of the insulating materials considered here are brittle. To ensure a uniformly distributed loading condition, a reinforced elastomer such as FABCO SA-47 bearing pad shall be used.

The insulator disc and the gradient plate shall be bonded with ABLEFILM 550 epoxy adhesive.

Materials

Platform. ASTM A-36 structural steel beams and plates with yield strength. σ_y = 36000 psi are considered. Weld rod E7018 shall be used.

Insulator Columns. Gradient Plate = Al 6061-T6 plate with yield strength, σ_{yt} = 3500 psi, σ_{yc} = 35000 psi, σ_{ys} = 20000 psi.

Insulating Disc

- Ceramics
- Glass
- Lexan
- Acrylic

The above materials shall be considered for the column-type platform. Due to the smaller size of the column, some of the brittle material can be considered because the loading on the disc is readily predictable. Based on materials shape, availability, and fabricating constraints only, acrylic sheet is considered for the flat-type platform. Detailed material properties are given in the following pages.

Table 7. Ceramic parameters.

HIGH ALUMINA CERAMICS *

Type (% alumina) →	85%	95%	99 + %
PHYSICAL PROPERTIES			
Specific Gravity.....	3.45	3.65	3.85
Ther Cond (200 F), Btu/hr sq ft/°F/ft....	8.5	12.1	14.5
Coef of Ther Exp, per °F			
77-390 F.....	3.1×10^6	3.7×10^6	——
77-750 F.....	3.7×10^6	4.0×10^6	——
77-1100 F.....	3.9×10^6	4.3×10^6	4.3×10^{-6}
77-1470 F.....	4.1×10^6	4.5×10^6	——
77-1830 F.....	4.3×10^6	4.7×10^6	——
Water Absorption, %....	0.0	0.0	0.0
Max Rec Svc Temp, F....	2460	3000	3540
ELECTRICAL PROPERTIES			
Dielec Str. v/mil.....	200	250	300
Dielec Const (77 F, 1 mc)	8.2	8.9	9.6
Power Factor (77 F, 1 mc)	0.0009	0.00035	0.00027
Loss Factor (77 F, 1 mc)	0.007	0.003	0.003
Te Value, F.....	1560	1960	2012
MECHANICAL PROPERTIES			
Mod of Elast in Ten, psi.	32×10^6	40×10^6	50×10^6
Ten Str, 1000 psi.....	20	30	39
Flex Str, 1000 psi.....	41	45	47
Compr Str, 1000 psi....	250	300	400
Hardness			
Mohs.....	9	9	9
Knoop.....	1450	1750	——
Impact Str (Charpy), in-lb	6.5	7.0	——

*The values given are not maximum values and are dependent upon the minor components or fluxes used as well as a number of other factors.

Table 8. Glass parameters.

Type	Borosilicate
Color	Clear
Forms Usually Available[a]	B,P,S,T,U
Specific Gravity	2.23
Refractive Index (Sod. D line)[b]	1.474
Impact Abrasion Resistance[c]	3.1
Young's Modulus, 10^6 psi	9.1
Polsson's Ratio	0.20
Thermal Expansion, 10^{-7} in/in/^oF[d]	18.1
Thermal Shock Res, Annealed[e]	
1/4 in. Thick, ^oF	26.6
Thermal Stress Res, ^oF[f]	97
Annealed, Normal Service, F	446
Annealed, Extreme Limit, F	914
Tempered, Normal Service, F	500
Tempered, Extreme Limit, F	554
Log^{10} of Vol. Res[g]	
77 F	15
662 F	6.6
Dielectric Properties at 1 Mc, 68 F	
Power Factor, %	0.50
Dielectric Constant	4.6
Loss Factor, %	2.6
Weathering[h]	1
Water[h]	1
Acid[h]	1

[a]Key: B= blown ware; M=multiform; U=panels; P=pressed ware; R=rolled sheet; LC=large castings; S=plate glass; T=tubing and rod. b) 0.5893 microns. c) Shows relative resistance to sandblasting. d) Range—32 to 572 F. e) Plates 6 in x 6 in: shows the temperature differenial a sample can experience without breakage when the sample is plunged into cold water after oven heating. f) Shows the temperature differential between the two surfaces of a tube of a constrained plate that will cause a tensile stress of 1000 psi on the cooler surface. g) In ohm-cm. [h]Key: 1=will virtually never show effects; 2=may occasionally show effects: 3=will probably show effects.

Table 9. Lexan parameters.

	Polycarbonates
Materials and Type →	Unfilled
PHYSICAL PROPERTIES	
Specific Gravity.	1.19-1.22
Retractive Index, n.	1.586
Transparency (visible light), %	85-89
MECHANICAL PROPERTIES	
Tensile Strength (yld), 1000 psi.....	8.5-9.0
Elongation (ult), %.....	90-115
Tensile Modules, 1000 psi.....	325-340
Flexural Strength, 1000 psi.....	12-13.5
Flexural Modulus, 1000 psi.....	310-345
Compressive Str[a], 1000 psi.....	10-12.5
Fatigue Str[b], 1000 psi	
10^4.....	5.4
10^5.....	2.0
10^6.....	1.0
10^7.....	0.8
Impact Strength	
Izod (notched), lb/in	12-16
Gardner, ft lb/in	—
Hardness	
Rockwell	M68-74
Shore	—
ELECTRICAL PROPERTIES	
Vol Res. ohm cm	8.2×10^{16}
Dielec Str, v/mil (dry)	
Short Time	380-425
Dielec Constant	
60 Hz	3.01-3.17
10 Hz	2.96-3.05
Dissip Factor	
60 Hz	0.0009
10 Hz	0.010
Arc Res. Sec (Lungsten Electrodes)	120
THERMAL PROPERTIES	
Ther Cond, Btu/hr/sq ft/^{o}F/in	1.35-1.41
Coef of Therm esp. 10 /ft	3.75
Specific Heat, Btu/lb/^{o}F	0.30
Heat Deflection Temp, F	
At 66 psi	280-290
At 264 psi	260-288
Brittleness Temp, F	-200
Max Temp Cont Use (No Load), F	—

Table 9. (cont.)

CHEMICAL AND ENVIRON RES	
Water absorption, %	
In 24 hr	0.15
Weathering	Discolors
Acids	
Weak	Resists
Strong	Attacks
Alkali	
Weak	Res-attacks
Strong	Attacks
Organic Solvents	Attacks
Fuels	Attacks
Oil and Grease	Resists
METHODS OF PROCESSING	Blow, foam, injection, rotational mldg; extrusion Thermoforming.

Table 10. Acrylic parameters.

Type →		General Purpose Type 1[a]
PHYSICAL PROPERTIES	ASTM	
Specific Gravity	D792	1.17-1.19
Ther Cond Btu/hr/sq ft/°F/ft		0.12
Coef of Ther Exp. 10^5		4.5
Spec Ht Btu/lb/°F	——	0.35
Refractive Index		1.485-1.500
Transmittance (Luminous,0.125 in), %	D791	91-92
Haze, %	D672	1-2
Water Absorption (24 hr), %	D570	0.3-0.4
MECHANICAL PROPERTIES		
Mod of Elast in Tension, 10^6 psi	D638	3.5-4.5
Ten Str, 1000 psi		6-9
Elong (in 2 in), %	D638	2-7
Hardness (Rockwell)	D785	M80-90
Impact Str (Izod notched), ft-lb/in	D256	0.4
Mod of Elast in Flex, 10 psi	D790	3.5-4.5
Flex Str, 1000 psi	D790	12-14
Compr Yld Str (0.1% offset), 1000 psi	D695	12-14
ELECTRICAL PROPERTIES		
Vol Res ohm cm	D257	$>10^{15}$
Dielec Str (Short Time), v/mil	D149	450-530
Dielec Const		
60 Cycles	D150	3.5-4.5
10 Cycles	D150	2.7-3.2
Dissip Factor		
60 Cycles	D150	0.05-0.06
10 Cycles	D150	0.02-0.03
Arc Resistance, sec		No track
APPLICABLE PROCESSING METHODS		Thermoforming, casting
CHEMICAL RESISTANCE		Resists weak alkalis, acids and aliphatic hydrocarbons. Attacked by esters, ketones, aromatic hydrocarbons, chlorinated hydrocarbons and concentrated acids.

Table 11. Specifications: FABCO SA Bearing Pads.

The preformed pads shall consist of a fabric and rubber body.

The pad shall be made with new unvulcanized rubber and unused fabric fibers in proper proportion to maintain strength and stability.

The surface hardness expressed in standard rubber hardness figures shall be 80 Shore A Durometer + or - 10 durometer average.

The ultimate breakdown limit of the pad under compressive loading shall be no less than 7,000 lbs. per square inch for the specified thickness without extruxion or detrimental reduction in thickness.

The pads shall be furnished to specified dimensions with all bolt holes accurately located.

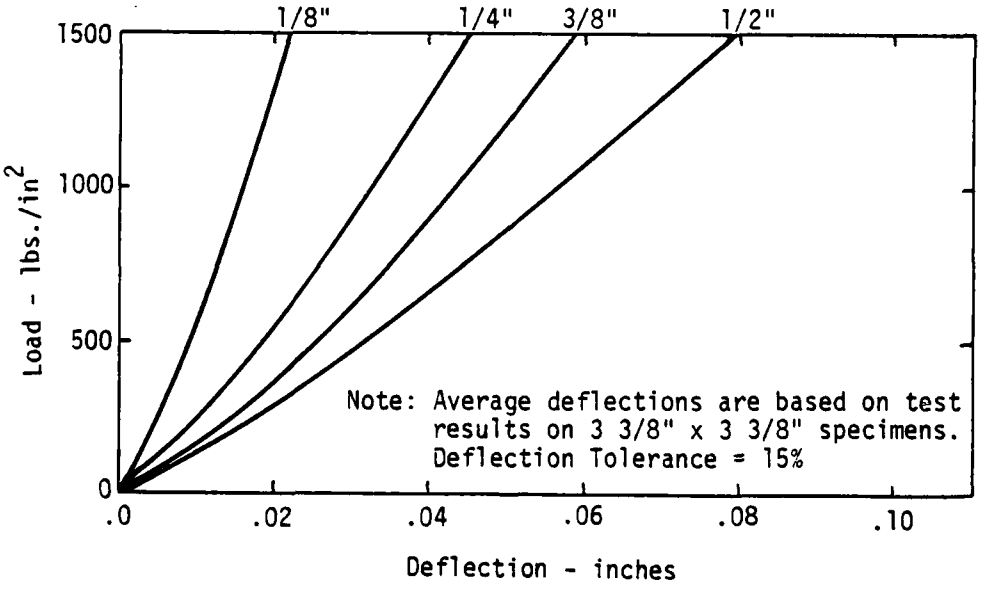

Table 12. Humidity resistant film adhesive for hermetic sealing of microelectronic packages.

Description: ABLEFILM 550 is a glass supported modified epoxy film adhesive. It was designed specifically for sealing of gold plated packages and exhibits greater adhesion before and after exposure to high humidity than any other known film adhesive. Although designed to overcome problems associated with the bonding of gold, adhesion to other materials used to make microelectronic packages is equally outstanding.

Advantages

Die Cut Preforms	ABLEFILM 550 can be furnished as die cut preforms to customer drawings.
Room Temperature Storage	The anticipated storage life of ABLEFILM 550 is six months at room temperature (25°C maximum). Refrigerated storage is recommended but not mandatory.
Moderate Temperature Cure	This adhesive can be cured at 150°C for two hours.
Excellent Adhesion to Gold	ABLEFILM 550 exhibits excellent adhesion and bond strength to clean gold surfaces. Shear strength to gold is 6000 psi.
Controlled Thickness Bonds	Bond thickness is accurately controlled to the thickness of the glass fabric carrier.
No Sticky Mess	ABLEFILM 550 is a tack-free adhesive. The use of this film adhesive eliminates the messy handling, clean-up and dermatitis characteristic to paste or liquid adhesives.

Table 12. (cont.)

Typical Properties

Color	Amber translucent
Carrier	Style 104 glass cloth
Volatile Content	Less than 0.5%
Suggested Care Cycles	2 hours @ 150°C or 1 hour @ 170°C

For many purposes a cure of 2 hours @ 125°C has been found adequate; however decreased moisture resistance on gold surfaces will result with this cure cycle.

Continuous Service Temperature (maximum)	125°C
De-Lidding Temperature	150°C
Temperature Cycling on Gold Plated Steel Lid (1 in.) bonded to glass, 10 cycles 125°C to -75°C	No failures

Tensile Shear Strength on gold plated stainless steel	
@ 25°C	6000 psi
@ 100°C	2800 psi
@ 125°C	1000 psi
@ 150°C	300 psi
@ 25°C after 20 days	
@ 85°C, 100% R.h.	2300 psi

Instructions for Use

A. Sealing (no hot purge cycle)

1. Place adhesive preform between clean package and lid.
2. Clamp with a spring clamp which will furnish a continuous force of approximately one pound during cure. A simple

Table 12. (cont.)

wooden clothes pin has been found generally suitable for most package sizes and configurations.

3. Place clamped package in a forced air oven preheated to 150°C and allow to cure for two hours.

B. Sealing (with hot purge cycle)

1. Place adhesive preform between clean package and lid.
2. Clamp with a spring clamp which will furnish a continuous force of one pound. Again, a simple wooden clothes pin has been found to be a suitable clamp device.
3. Place clamped package in a vacuum oven preheated to the desired purge temperature (100°C or less).
4. Evacuate the oven and hold the vacuum for any desired time up to 15 minutes.
5. Release vacuum and back-fill with inert gas.
6. Increase oven temperature to 150°C and cure for two hours.

Availability: ABLEFILM 550 is available as die cut preforms dimensioned to customer drawings. This adhesive is supplied on a 1-mil-thick open weave glass carrier. Total film thickness is in the range of 3 mils to 8 mils (±0.5 mill). Other carrier thicknesses and total film thicknesses may be available on request.

Caution: Although this product is considered essentially non-toxic, it could conceivably cause dermatitis to persons exhibiting an extreme sensitivity to epoxy resins or amine hardeners. Persons having this sensitivity should avoid skin contact. If contact does occur, wash affected area immediately with soap and water.

Storage: The shelf life of ABLEFILM 550 at room temperature is six months. Under standard refrigeration (+5°C) shelf life is nine months, and at -40°C, one year. Die cut preforms must be stored under standard refrigeration (+5°C or colder).

Table 12. (cont.)

Disclaimer: All statements, technical information and recommendations contained herein are based on tests we believe to be accurate, but the accuracy or completeness thereof is not guaranteed, and the following is made in lieu of warranty express or implied: Seller and manufacturer's only obligation shall be to replace such quantity of the product proved to be defective. Neither seller nor manufacturer shall be liable for any injury, loss or damage, direct or consequential, arising from the use of inability to use the product. Before using, user shall determine the suitability of the product for his intended use, and user assumes all risk and liability whatsoever in connection herewith. No statement or recommendation not contained herein shall have any force or effect unless in agreement signed by officers or seller and manufacturer.

Stress Analysis

Column-Type Platform Geometric Dimensions*

Refer to Figures 2.8 and 2.9, Section 2.

Platform

Longitudinal Beam

Nose gear--maximum bending moment, $M_N = \frac{F_M \ell_M}{4}$

$= \frac{46,500 \times 100}{4}$

$= 1,162,500$ lb-in.

Main gear--maximum bending moment, $M_M = \frac{F_M \ell_M}{4}$

$= \frac{46,500 \times 120}{4}$

$= 1,395,000$ lb-in.

*Refer to Boeing 747, D6-14043, Section 3, pp. 45, 68.

Consider a 12 WF 72 lb/ft beam.

$$I = 597.4 \text{ in.}^4$$

$$S = 97.5 \text{ in.}^3$$

Bending Stress, $\sigma_b = \frac{M_M}{S} = 14{,}310$ psi

Deflection check, $\delta = \frac{F_M \ell_M^3}{48\ EI} = \frac{46{,}500 \times 120^3}{48 \times 30 \times 10^6 \times 597.4}$

$$= 0.093 \text{ in.}$$

Transverse Beam

Maximum beam loading (main gear):

Wheel spacing, $a_M = 58$ in.

Column spacing, $\ell_M = 120$ in.

$$F = F_M \left(2 - \frac{a}{\ell}\right)$$

$$= 46{,}500 \left(2 - \frac{58}{120}\right)$$

$$= 70{,}525 \text{ lb.}$$

Maximum bending moment,

$$M = \frac{F}{2} (b - 50)$$

$$= \frac{70{,}525}{2} (72-50)$$

$$= 775{,}775 \text{ lb-in.}$$

Maximum bending stress,

$$\sigma_b = \frac{M}{S} = \frac{775{,}775}{97.5} = 7957 \text{ psi}$$

Using 12 x 12 WF 72 lb/ft beam for main framing is adequate.

Insulator Column

Maximum Column Load

$$F_c = F_M \left(2 - \frac{a_M}{\ell_M}\right) + \frac{W_S}{4}$$

$$= 46{,}500 \left(2 - \frac{58}{120}\right) + \frac{8000}{4}$$

$$= 72{,}525 \text{ lb}$$

Consider a 10-inch-diameter bearing surface. The average compressive stress in the column is:

$$\sigma_c = \frac{72525}{\frac{\pi}{4}(10)^2} = 923.4 \text{ psi}$$

Maximum Shear Load in Column

(a) F_{MA} = 7440 lbs (due to towing)
Shear stress (60% bonding efficiency)

$$\sigma_s = \frac{F_{MA}}{\alpha A} = \frac{7440}{0.6 \times \frac{\pi}{4}(10)^2} = 157.8 \text{ psi}$$

(b) Column shear due to wind. Assume wind load is resisted by main gear platform only; then average shear load per column is

$$F_\ell = \frac{F_L}{16} = \frac{94050}{16}$$

$$= 5878 \text{ lbs} < 7440 \text{ lbs}$$

$$\sigma_s = \frac{5878}{0.6 \times \frac{\pi}{4}(10)^2} = 124.7 \text{ psi}$$

Since the slenderness ratio of this column is much smaller than 40, there is no elastic instability problem.

Flat-Type Platform

Insulating material considered: Acrylic top bearing plate: 2-in,-thick steel plate.

Top bearing plate and insulating plate interface pressure:

Foundation Modules,

$$k = \frac{E_a}{\ell_a} = \frac{3 \times 10^5}{40} = 7.5 \times 10^3 \text{ lb/in.}^3$$

Foundation Damping Factor,

$$\beta = 4\sqrt{\frac{3k}{E_s t_s^3}}$$

$$= 4\sqrt{\frac{3 \times 7.5 \times 10^3}{30 \times 10^6 \times 2^3}}$$

$$= 0.0983$$

Interface Pressure,

$$\rho(x) \approx 0.5\ p\ e^{-\beta x} \cos \beta x$$

try $x = 10$ in. $P(10) = 0.103\ \rho_o$

This result indicates 2-inch-thick plate will redistribute the wheel loads somewhat.

Wheel and Plate Interface Bearing Area,

$$A \approx 15 \text{ in.} \times 25 \text{ in.} = 375 \text{ in.}^2$$

Maximum Wheel Loading

$$F_N = 46850 \text{ lb}$$

Therefore, $P_o = \frac{F_N}{A} = 125$ psi

$P_o << \sigma_c = 12000$ psi, ultimate compression strength of acrylic.

Acrylic insulator will not be damaged.

Acrylic/Ground Interface:

Radius of relative stiffness,*

$$r = 4\sqrt{\frac{E_a \ell_a^3}{12\,(1 - \nu^2)\,k}}$$

$$= 4\sqrt{\frac{3 \times 10^5 \times 40^3}{12\,(1 - 0.3^2)\,7.5 \times 10^3}} = 22.0 \text{ in.}$$

Insulating Platform Deflection:

$$\delta = \frac{2F_N \ell_a}{(\pi r^2 + A)\,E_a}$$

$$= \frac{2 \times 46850 \times 40}{(\pi \times 22^2 + 375)\,3 \times 10^5}$$

$$= 0.0066 \text{ in.}$$

This deflection is small enough that the acrylic sheets will not undergo desired bending stresses due to moving load. Since the large-area acrylic sheets and the gradient plates are bondedm the lateral shear stresses can be neglected for this type of the platform.

Discussion

The following tables list the advantages and disadvantages of the platforms considered, and stress summary for the column type platform.

*Refer to "Concrete Pavement Design," Portland Cement Association, Chicago, 1951

Table 13. Comparison of column and flat type platforms.

	Advantages	Disadvantages
Column Type	•Lighter weight •Insulating column quality control is better due to smaller size •Broader choice of insulating material	•Potential column buckle due to severe dielectric breakdown
Flat Type	Structural integrity is not affected by severe dielectric breakdown	•Heavier weight •Platform may not be flat; requires shiming •Choice of insulating material is limited

Table 14. Stress summary for column type platform.

	Item	Loading Condition	Stress Level (psi)	M.S.	Remarks
Platform	Longitudinal Beam 12 WF 72	Wheel Loading	14,310	4.17	OK
	Transverse Beam 12 WF 72	Wheel Loading	7,960	8.29	OK
Insulator Column	Gradient Plate 1/4''∿1/2'' thick 11''ϕ	Column Comp.	925	44.5	OK
		Towing	158	169.8	OK
		Wind	125	215.0	OK
	Bonding Agent ABLEFILM 550	Towing	158	36.9	OK
	Ceramic	Column Comp.	925	>300.0	OK
		Towing	158	>400.0	OK
	Glass	Column Comp.	925	98.0	OK
		Towing	158	114.0	OK
	Lexan	Column Comp.	925	9.8	OK
		Towing	158	29.1	OK
	Acrylic	Column Comp.	925	11.9	OK
		Towing	158	20.2	OK

$$M.S. = \frac{\sigma_{ultimate}}{\sigma_{working}} - 1$$

CONCLUSIONS AND SUMMARY

Two versions of a dielectric stand coupled with Freon insulation are presented. Each of these versions will allow application of a 3 MV pulse with a one microsecond risetime and a 50 microsecond e-fold falltime to three types of aircraft designated for the study--E-4B, EC-135, and EC-130.

During the course of the study, several methods of aircraft EMP isolation were considered in addition to the chosen method. Two of the more interesting methods will be briefly discussed.

Because of the contract instructions to avoid solutions involving high dielectric stands and because of the very high dielectric strength of homogeneous solid insulators, one of the earliest concepts was a large-area but very low solid dielectric stand approximately one foot in height. The electric field and the top of the stand would then be 100 kV/cm. Such a field would break down even the strongest of dielectric gases; therefore, a large area is required to voltage-grade the region around the aircraft landing gear in order to prevent flashover. It was immediately realized that there would be serious problems with this approach due to the phenomenon of traveling sparks. When an electrode is placed on a dielectric sheet over a ground plane and the electrode is raised above the breakdown point of the surrounding gas, traveling sparks run toward the edges of the insulator. These sparks are driven very energetically by the discharge of the fringing capacitance and will travel for a very long distance. One method considered for handling the traveling spark problem was to surround the low dielectric stand by concentric dams. The intervening regions between dams would be filled with mineral oil. Each dam would be higher as the outer edge of the concentric array is approached until the height of the final dam is sufficient to hold the voltage in Freon. Accurate analysis of such a system is difficult, and the idea was eventually given up as being too elaborate and too costly. In addition, EMP simulation performed on a system using the large-area approach would be dominated by the support stand capacitance, which distorts currents flowing on the aircraft.

The second idea that has not yet been discussed is of potentially more interest. This idea involves the use of a metallic grading platform placed under the wheels of the aircraft and supported by an inflatable bladder filled with Freon or SF_6. For the E-4B aircraft, the pressure required was computed to be 7.5 psig, and the thickness of the rubber bladder was required to be 1.486 cm. Such a support system would not be stable against wind loads, and the aircraft would have to be guyed with dielectric ropes to afford wind stabilization. The required height of the gas-supported platform would have to be about the same as the solid dielectric stands chosen for presentation in this study (137.16 cm). The inflatable bladder was not studied extensively because certain aspects of the problem were difficult to evaluate (e.g., the consequences of puncturing the bladder with the high voltage pulse). In addition, a much larger engineering study than was possible on this contract is required to determine whether such an idea is truly feasible.

In the course of the program, all of the essential requirements of the contract were accomplished.

The flashover of unspecified but field-enhanced shapes was determined for sea level and 1.52 km altitudes. The benefits derived by using high dielectric strength gases were determined, and a method of containing the gases is described.

Methods of achieving uniform fields were studied in order to design a dielectric stand of the lowest reasonable height. The uniform field methods were described and used in the two designs that are presented.

One version, the column type, is lighter than the other, the flat type, but the lighter column-type version is one foot higher than the more massive flat-type version.

Structural analysis of both designs was performed. The analysis included stress analysis for vertical loacs, lateral wind loads, and lateral towing loads. Both designs were shown to be structurally sound.

Dielectric materials were examined for possible use with both stand designs. Data on the various dielectric materials are presented.

The use of the dielectric stands and Freon-filled bags is illustrated for each of the contract specified aircraft--the E-4B, the EC-135, and the EC-130.

REFERENCES

1. Ward, A. L., "Calculation of Electrical Breakdown in Air at or Near Atmospheric Pressure, " Phys. Rev. Vol. 138, No. 5A, May, 1965.

2. Longley, H. J. and C. L. Longmire, Electron Mobility and Attachment Rate in Moist Air, MRC-N-222 (DNA 3856T), Mission Research Corporation, December, 1975.

3. Martin, J. C., "Nanosecond Pulse Techniques," AFWL PEP Note 4, April, 1970.

4. Crewson, W. F., "Operating Theory of Point-Plane Spark Gaps," AFWL Switching Note 11, March, 1971.

5. Martin, J. C., Million Volt Repetitive Spark Gaps, Proc. of the workshop on Switching Requirements and R&D for Fusion Reactors, EPRI-ER-376-SR, AWRE, Aldermaston, U. K., July, 1977.

6. Martin, J. C., "High-Speed Breakdown of Small Air Gaps in Both Uniform Field and Surface Tracking Geometrics," AFWL Switching Note 24.

7. Martin, J. C., "Pressure Dependency of the Pulse Breakdown of Gases," AFWL Dielectric Strength Note 15, September, 1967.

8. Martin, J. C., "D. C. Breakdown Voltages of Non-Uniform Gaps in Air," AFWL Dielectric Strength Note 16, June, 1970.

9. Buntschuk, C. and M. Gilden, "Nanosecond-Pulse Breakdown Study at Microwave Frequencies," AFWL Dielectric Strength Note 22, July, 1964.

10. Baum, C. E., et. a., "A Simple Way of Simulating the EMP Effects of the VLF/LF Dual-Wire Antenna on the E-4," AFWL Miscellaneous Simulator Memos, No. 14, November, 1977.

11. Tse, F. Y., et. al., "A Review of Dielectric Media - Liquid Insulation," Insulation/Circuits, January, 1971.

12. Bell, W., et. al., "A Review of Dielectric Media - Solid Insulation," Insulation/Circuits, December, 1970.

13. Bolin, P., et. al., "A Review of Dielectric Media - Vacuum Insulation," Insulation/Circuits, September, 1970.

14. Mulcahy, M. J., et. al., "A Review of Insulation Breakdown and Switching in Gas Insulation," Insulation/Circuits, August, 1970.

REFERENCES (Continued)

15. Alston, L. L., High Voltage Technology, Oxford University, Press, 1968.

16. Meek and Craggs, Electrical Breakdown of Gases, Oxford University, Press, 1953.

17. Felsenthal, P. and J. M. Proud, "Nanosecond-Pulse Breakdown in Gases," Phys. Rev., Vol. 139, No. 6A, September, 1965.

APPENDIX
PHYSICAL DIMENSIONS OF AIRCRAFT
E4-B, EC-135 and EC-130

This section presents the physical dimensions of the three aircraft considered for EMP Isolation Study. Besides the principal dimensions of these aircraft (such as the length of the fuselage, wings, etc), the ground clearances of the antennas under the fuselages, their dimensions, and the main and front landing gear features are pointed out. Appropriate figures are included to show the critical components for the isolation purposes and their dimensions. Some of the figures presented here are not to the scale.

1. E-4B DIMENSIONS

Overall dimensions of a 747-200B aircraft are shown in Figure A1. This figure is helpful as far as the design features of the dielectric platforms/ stands are concerned.

Figure A2 shows some of the under-fuselage and landing gear components of an E-4B aircraft. Many antennas are not shown in this figure; however, Figure A3 shows all the antennas on this aircraft. Table A1 shows the ground clearances and lengths of the most important components of E-4B for isolation study. Components listed in Table A1 can be located on Figure A3.

2. EC-135 DIMENSIONS

Table A2 shows the principal dimensions of the EC-135 aircraft; together with the gross weight and surface areas on the aircraft.

The nose landing gear (steerable dual wheel) retracts directly forward and into the wheel well in the lower nose compartment.

The main landing gear (two four-wheel) retracts laterally inboard to the wheel wells in the fuselage.

Figure A4 and A5 show the principal dimensions of EC-135 (some of which are tabulated in Table A2).

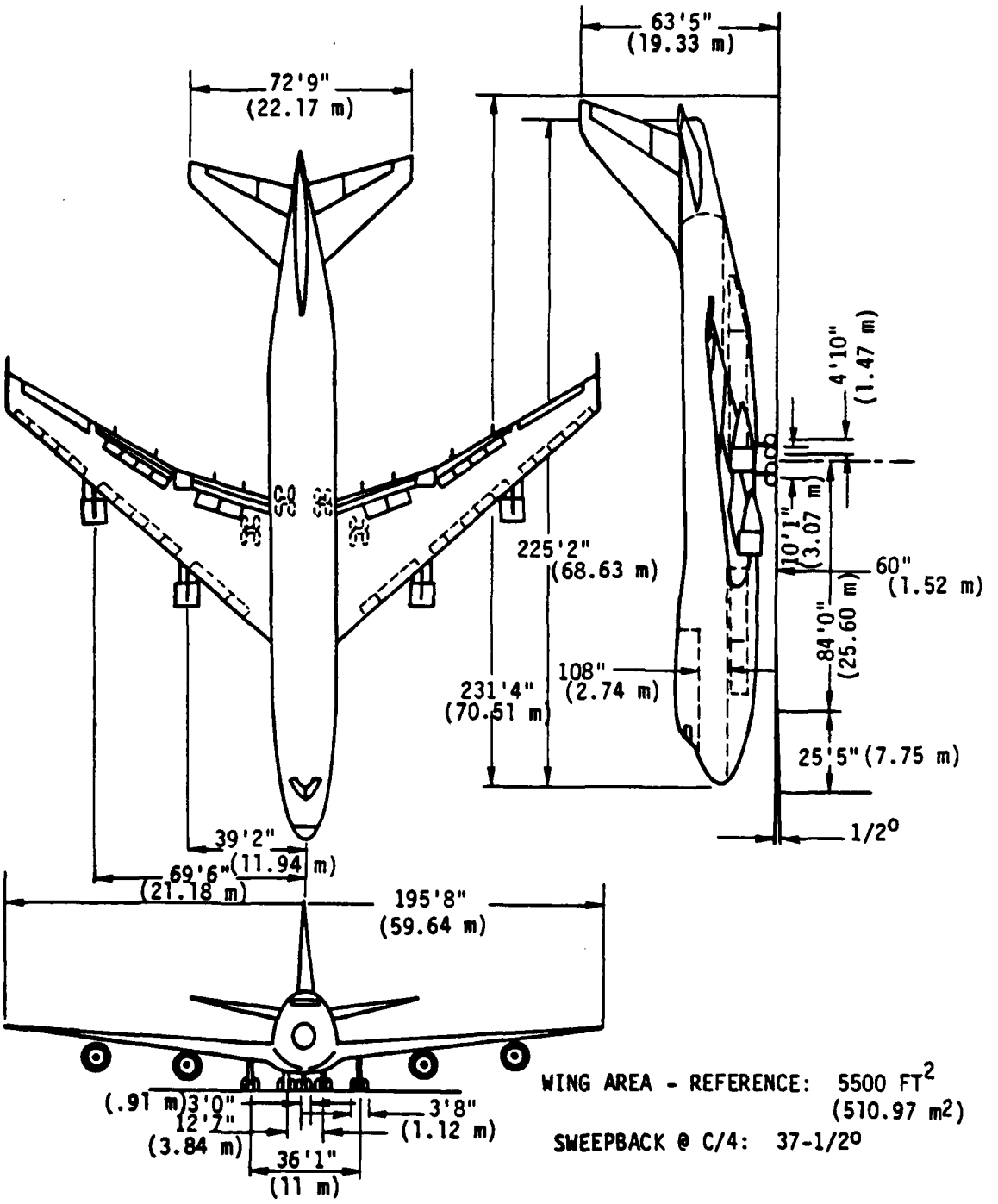

Figure A1. 747-200B dimensions.

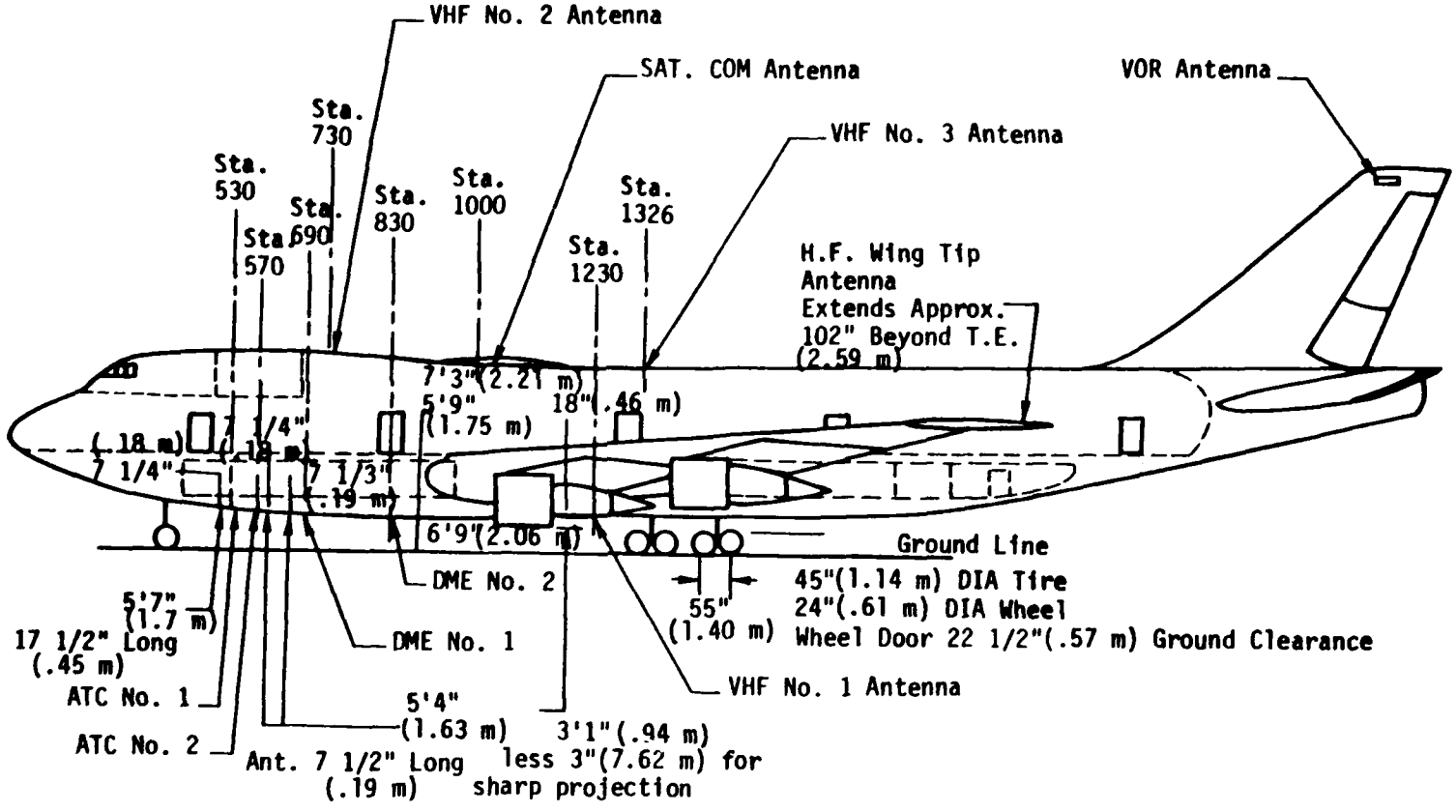

Figure A2. Ground clearance (antennas).

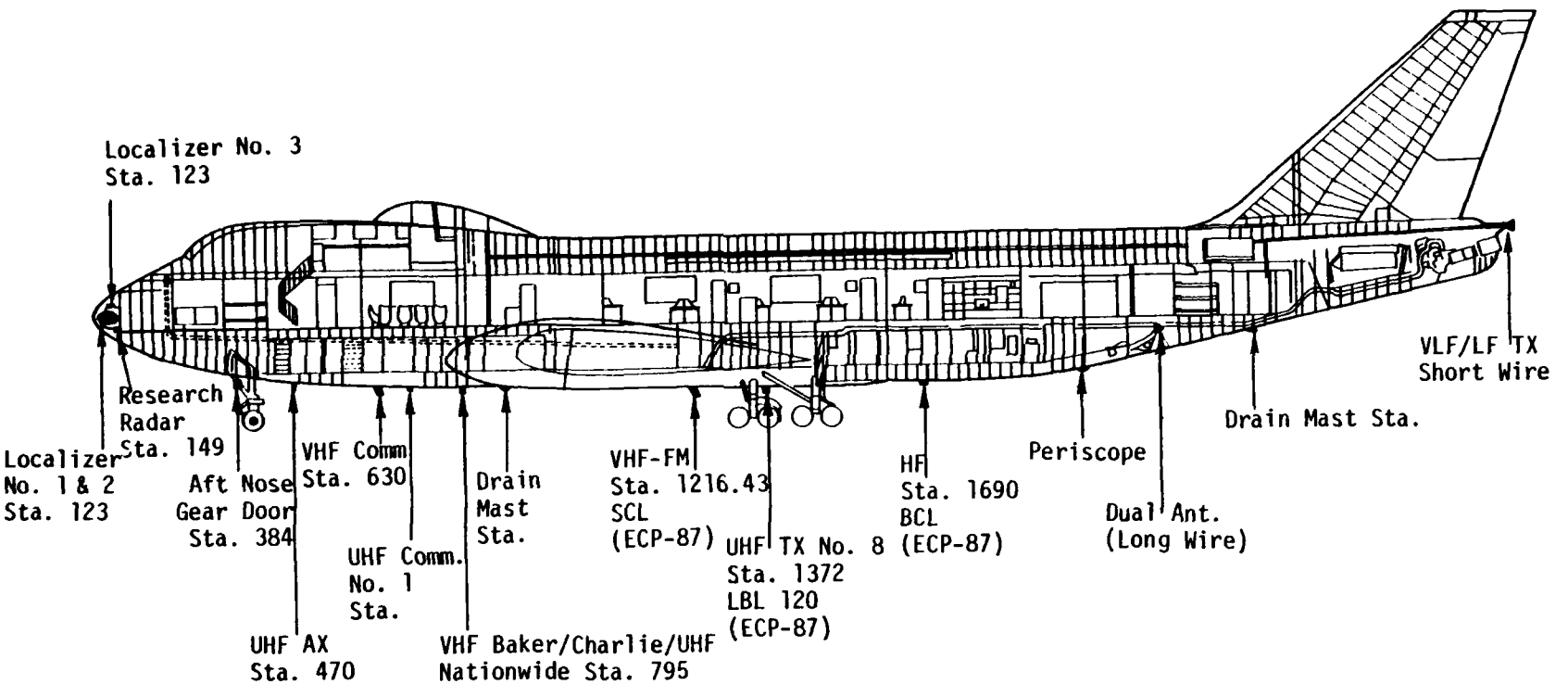

Figure A3. E-4B antennas.

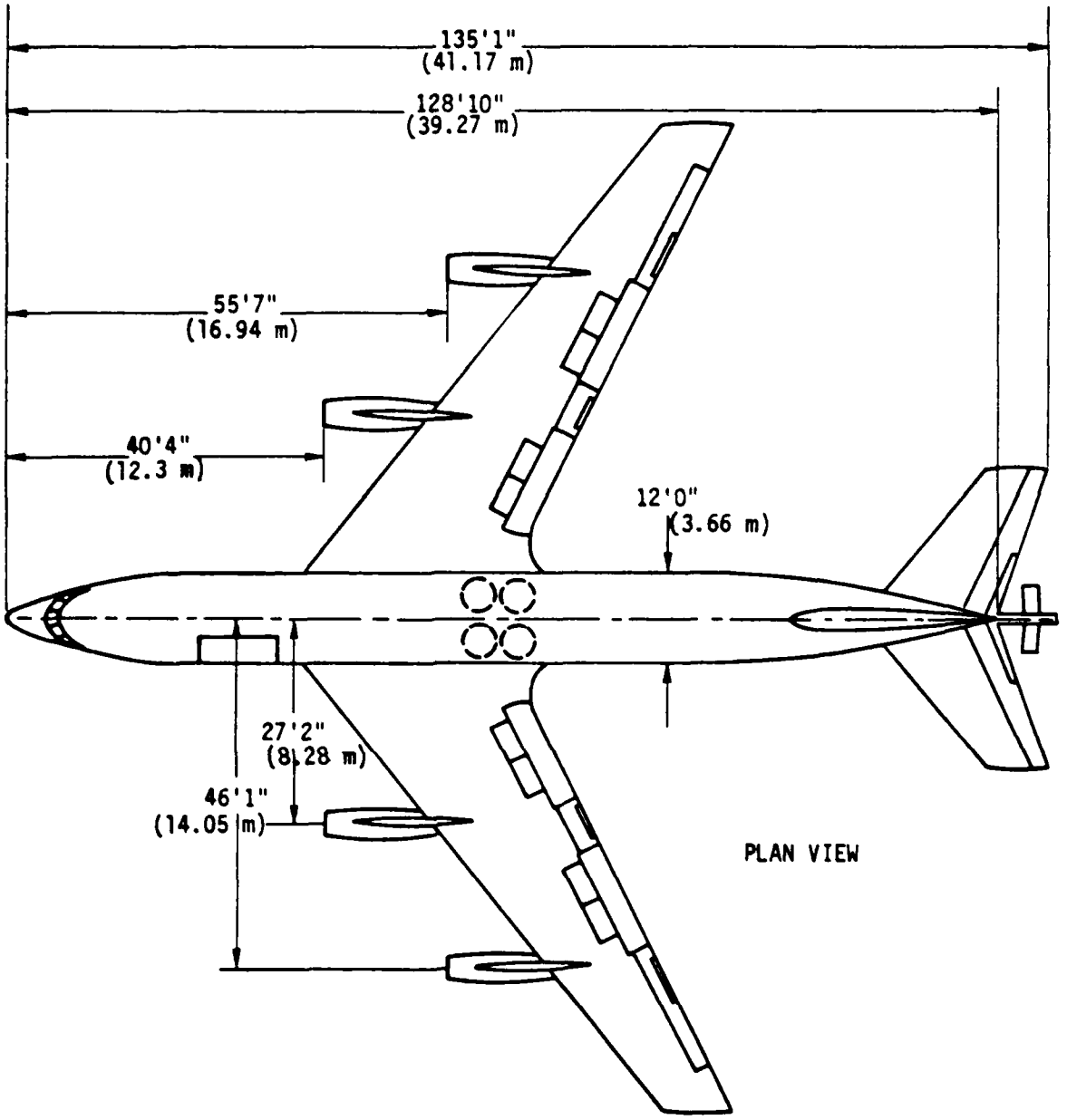

Figure A4. Principal dimensions of EC-135.

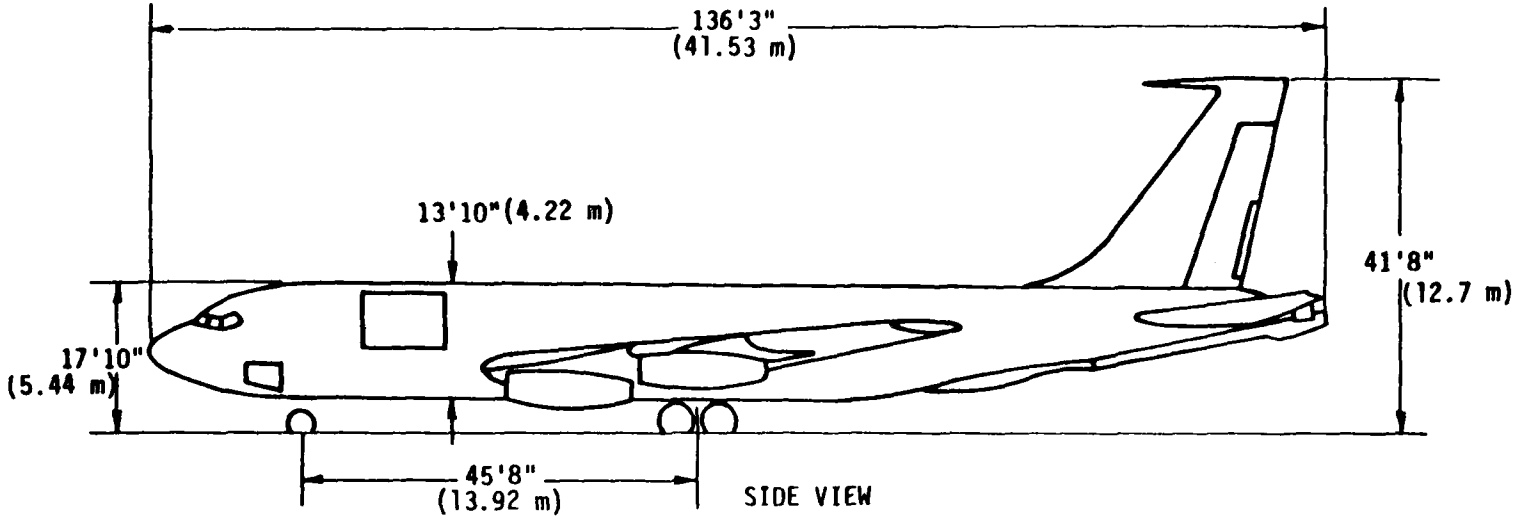

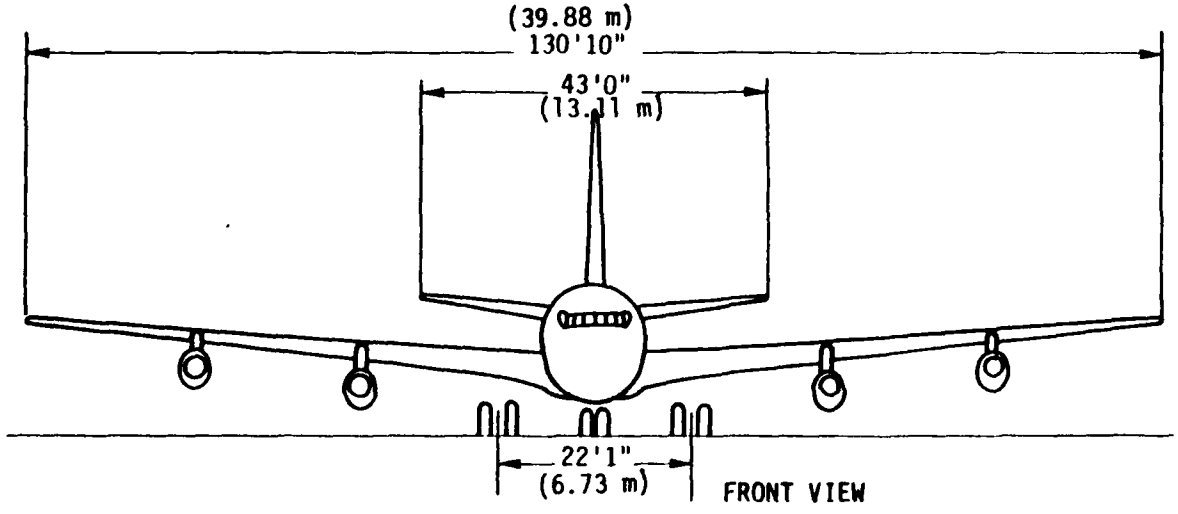

Figure A5. Principal dimensions of EC-135.

TABLE A1. POTENTIAL BREAKDOWN LOCATIONS ON E-4B (LOWER FUSELAGE)

Component	Height from Ground (m)	Length (m)
Nose	5.3	----
Aft nose gear door STA 364	1.8	----
UHF RX STA 470	1.9	0.18
VHF Comm STA 630	1.5	0.45
UHF Comm No. 1 STA 690	1.7	0.20
VHF Baker/Charlie/UHF Nationwide STA 790	1.5	0.30
Drain Mast STA 867.1	1.7	0.20
VHF-FM STA 1216.43 BCL (ECP-87)	1.3	0.45
UHF TX No. 5 STA 1372 LBL 13.0 (ECP-87)	1.7	0.18
MF STA 1690 BCL (ECP-87)	1.9	----
Periscope	2.5	----
Dual Ant (Long Wire)	2.6	0.80
Drain Mast STA 2308.59	4.2	0.20
VLF/LF TX (Short Wire)	8.9	0.40

Table A2. Principal dimensions of EC-135.

GENERAL	
Span	130 feet 10 inches (39.88 m)
Overall Length (not including boom)	135 feet 1 inch (41.17 m)
Height	41 feet 8 inches (12.7 m)
Height (fin folded)	19 feet 7 inches (5.97 m)
Centerline to Inboard Nacelle	27 feet 2 inches (8.28 m)
Inboard Nacelle Clearance (average)	24 inches (.61 m)
Centerline to Outboard Nacelle	46 feet 1 inch (14.05 m)
Outboard Nacelle Clearance (average)	49 inches (1.25 m)
Maximum Gross Weight - Taxi	301,600 pounds
WINGS	
Type	low
Airfold Section	BAC 310, 311, 312, 313
Chord at Root	337.98 inches (8.59 m)
Chord Near Tip	112 inches (2.85 m)
Mean Aerodynamic Chord	241.88 inches (6.14 m)
Incidence	2 degrees
Dihedral	7 degrees
Sweepback (at 1/4 chord)	35 degrees
Aspect Ratio	7.065
Wing Tip to Ground	15 feet (4.57 m)

Table A2. (cont.)

STABILIZER	
Span	43 feet 0 inches (13.11 m)
Maximum Chord	214.24 inches (5.44 m)
Incidence (normal)	8 degrees down
Dihedral	7 degrees
FIN	
Height	24 feet (7.32 m)
Base Chord	20 feet 2 inches (6.15 m)
Angle of Sweepback (leading edge)	36 inches 10 minutes
FUSELAGE	
Maximum Width	12 feet (3.66 m)
Maximum Height	17 feet 10 inches (5.44 m)
Height from Ground	4 feet (1.22 m)
Overall Length	128 feet 10 inches (39.27 m)
Height of Entry Door Above Ground	5 feet 4 inches (1.63 m)
Dimensions of Entry Door	
Height	40 inches (1.02 m)
Width	49 inches (1.25 m)
Height of Cargo Door Above Ground	10 feet (3.05 m)
Dimensions of Cargo Door	
Height	6 feet 6 inches (1.98 m)
Width	9 feet 9 inches (2.97 m)

Table A2 (cont.)

AREAS	
Wings (less ailerons)	2313.4 sq. ft. (214.92 m^2)
Wings (with flaps extended)	2754.5 sq. ft. (255.90 m^2)
Ailerons (total)	119.6 sq. ft. (11.11 m^2)
Main Flaps (total)	361.6 sq. ft. (33.59 m^2)
Leading Edge Flaps (total)	26 sq. ft. (2.42 m^2)
Stabilizer (including elevators)	545 sq. ft. (50.63 m^2)
Elevators (total including tab)	125.6 sq. ft. (11.67 m^2)
Elevator Tabs (total)	11 sq. ft. (1.02 m^2)
Fin (including rudder)	328.3 sq. ft. (30.50 m^2)
Rudder (including tab)	102.8 sq. ft. (9.55 m^2)
Rudder Tab	7.29 sq. ft. (0.68 m^2)

Due to the limited information that could be obtained from the aircraft technical orders, MRC made a trip to SAC Headquarters in Omaha, Nebraska where an EC-135 is lacated. The following detailed data was obtained by actual measurement of the aircraft during that visit.

The EC-135 studied was of C series, I.E., and EC-135. It had the wing fuel tanks full, and body fuel tanks partially full. Its gross weight was 264.1 kilopoinds with 120 kilopoinds of fuel. Due to the full wing tanks, the whole wing and the two engines had the minimum heights from the ground.

Figure A6 shows the dimensions of the front landing gear.

The front wheel doors can be disconnected to reduce the possibility of arcing during the testing.

Figure A7 shows the main landing gear (altogether 8 tires) dimensions. Like the front wheel doors, the main landing wheel doors can be disconnected for isolation considerations.

Figure A8 shows the bottom fuselage of EC-135. The letters A to F indicate the antennas.

The following figure, Figure A9, shows the antennas and their dimensions under the fuselage of the EC-135 aircraft. These are the antennas that are illustrated on Figure A8.

Figure A10 shows the mid and aft bottom fuselage antennas and the drain mast.

When the wing fuel tanks are full, the inboard engine ground clearance is .71 m and that of the outboard engine is 10.2 cm.

3. EC-130 DIMENSIONS

The subsection presents the principal dimensions, antenna dimensions and the ground clearance of various components of the EC-130 aircraft. Figure A11 shows the principal dimensions of the aircraft when the aircraft is equipped and empty.

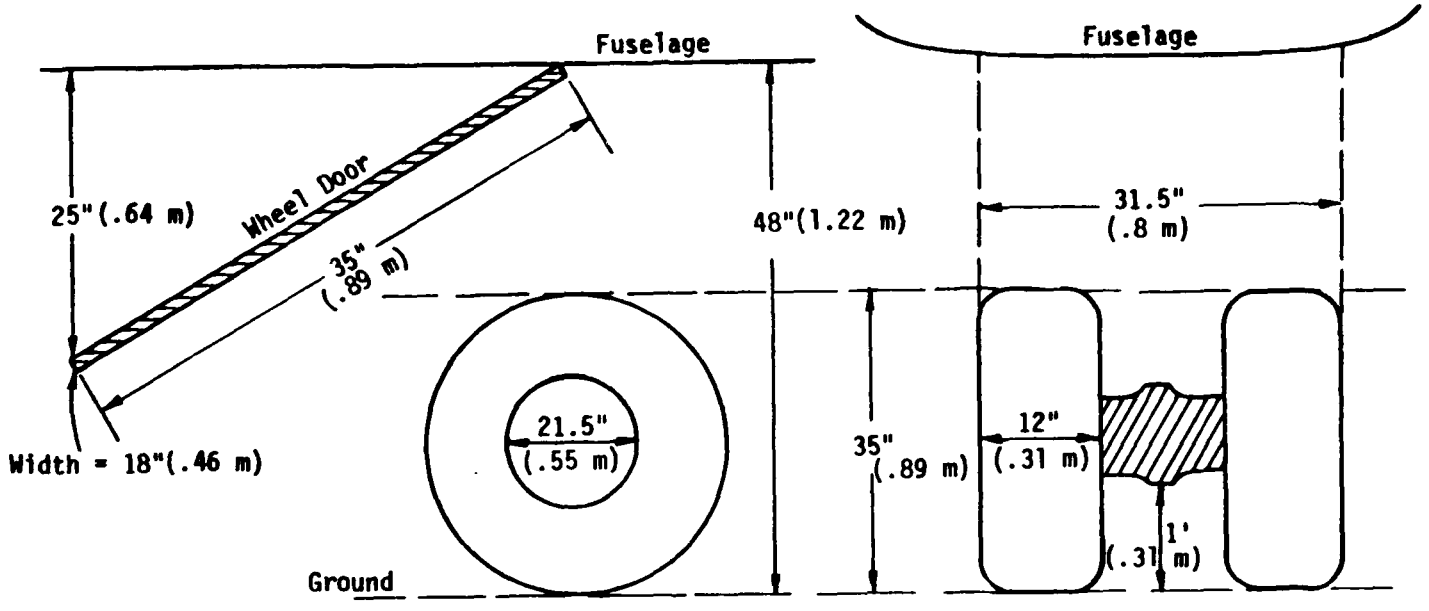

Figure A6. Front landing gear (dual tire).

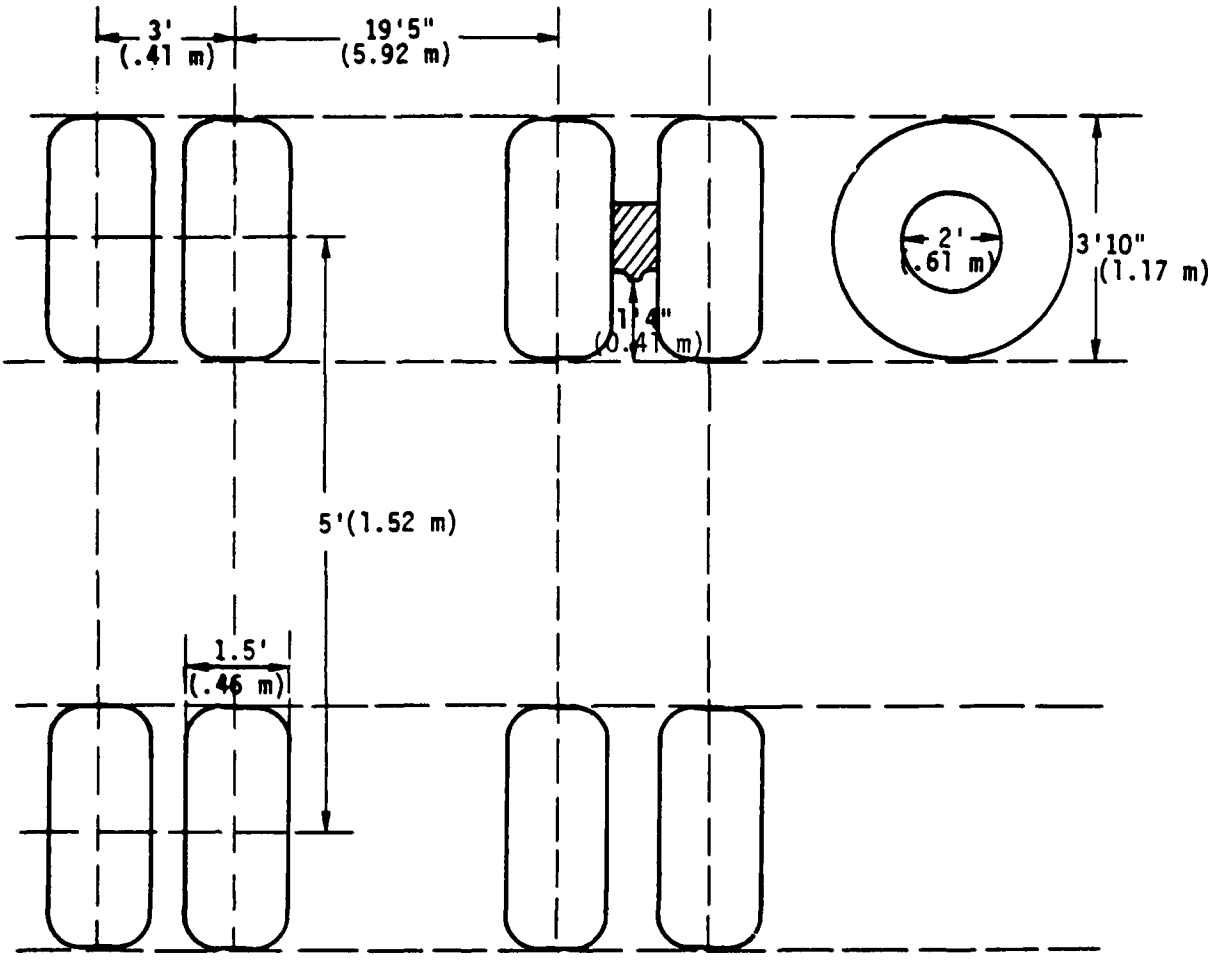

Figure A7. Main landing gear.

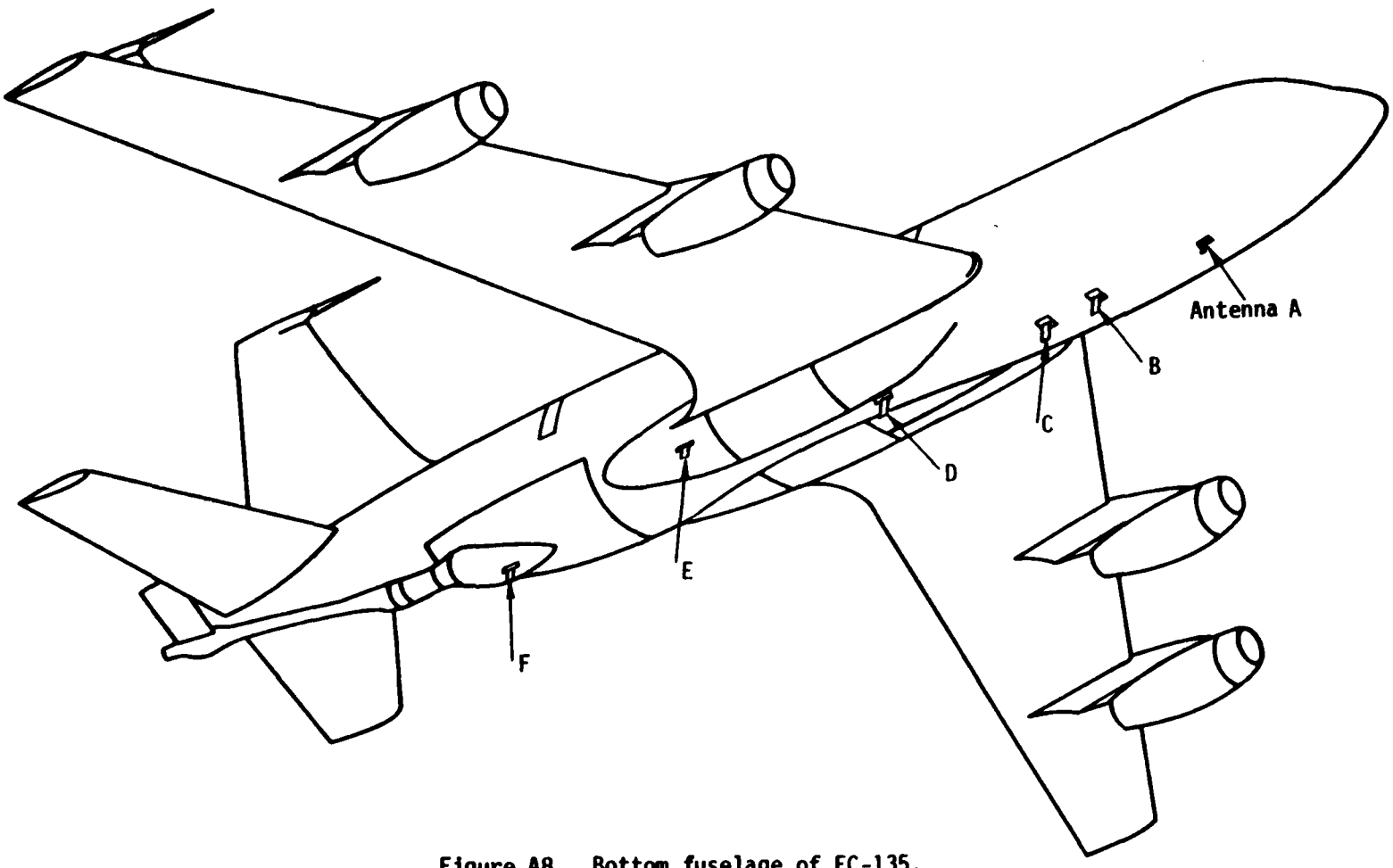

Figure A8. Bottom fuselage of EC-135.

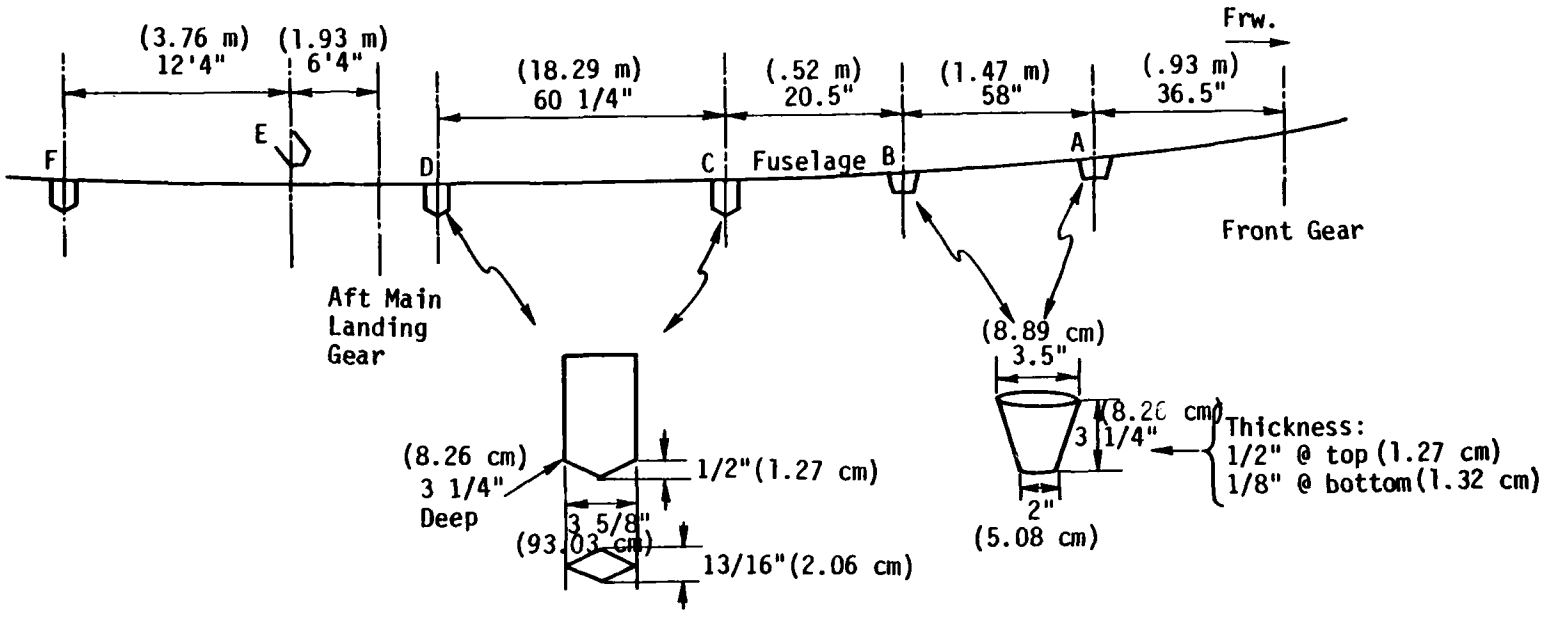

Note: Antennas C, D, E and F have the same dimensions.

Figure A9. Dimensions of EC-135 antennas.

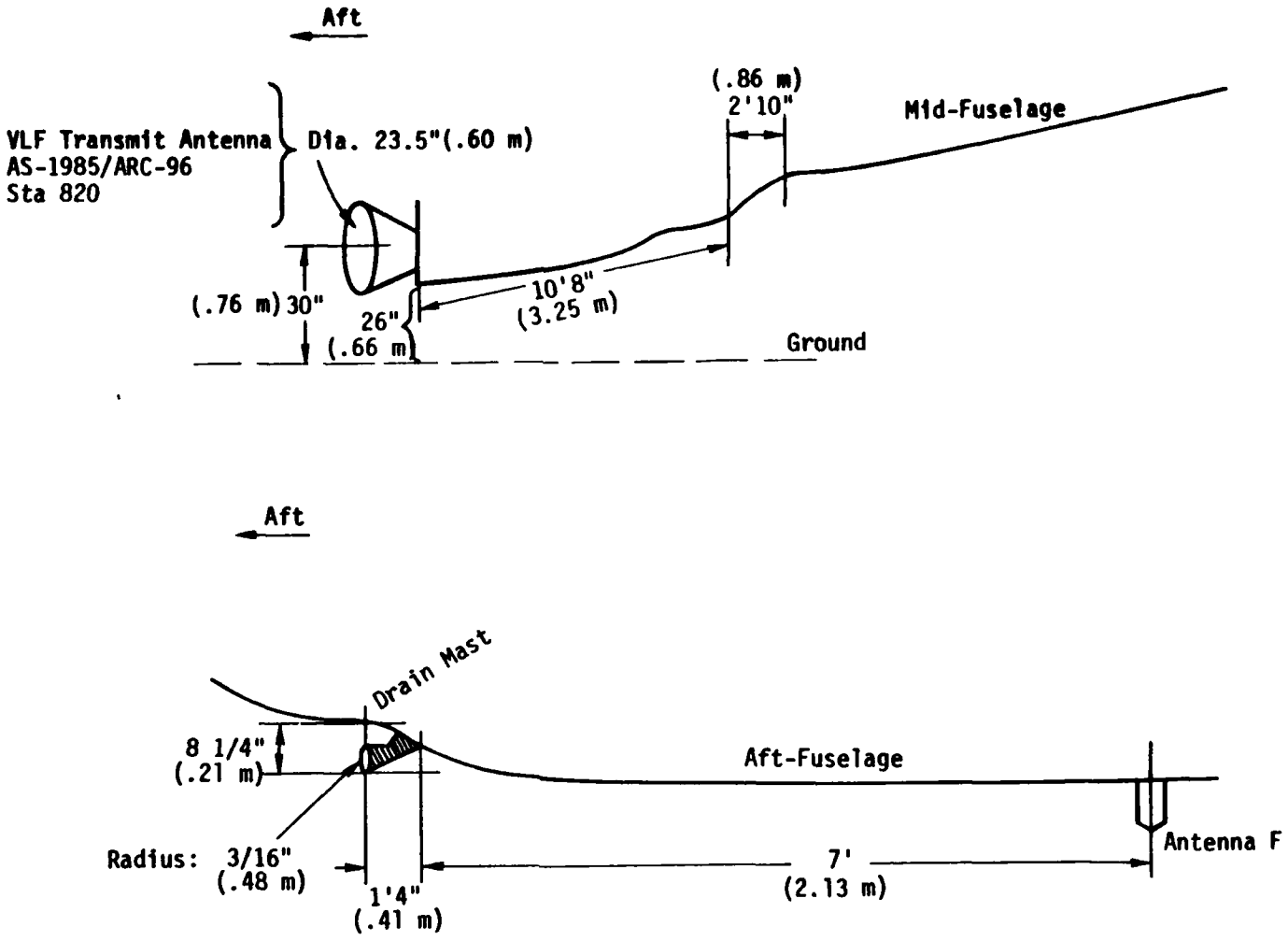

Figure A10. Bottom fuselage of EC-135.

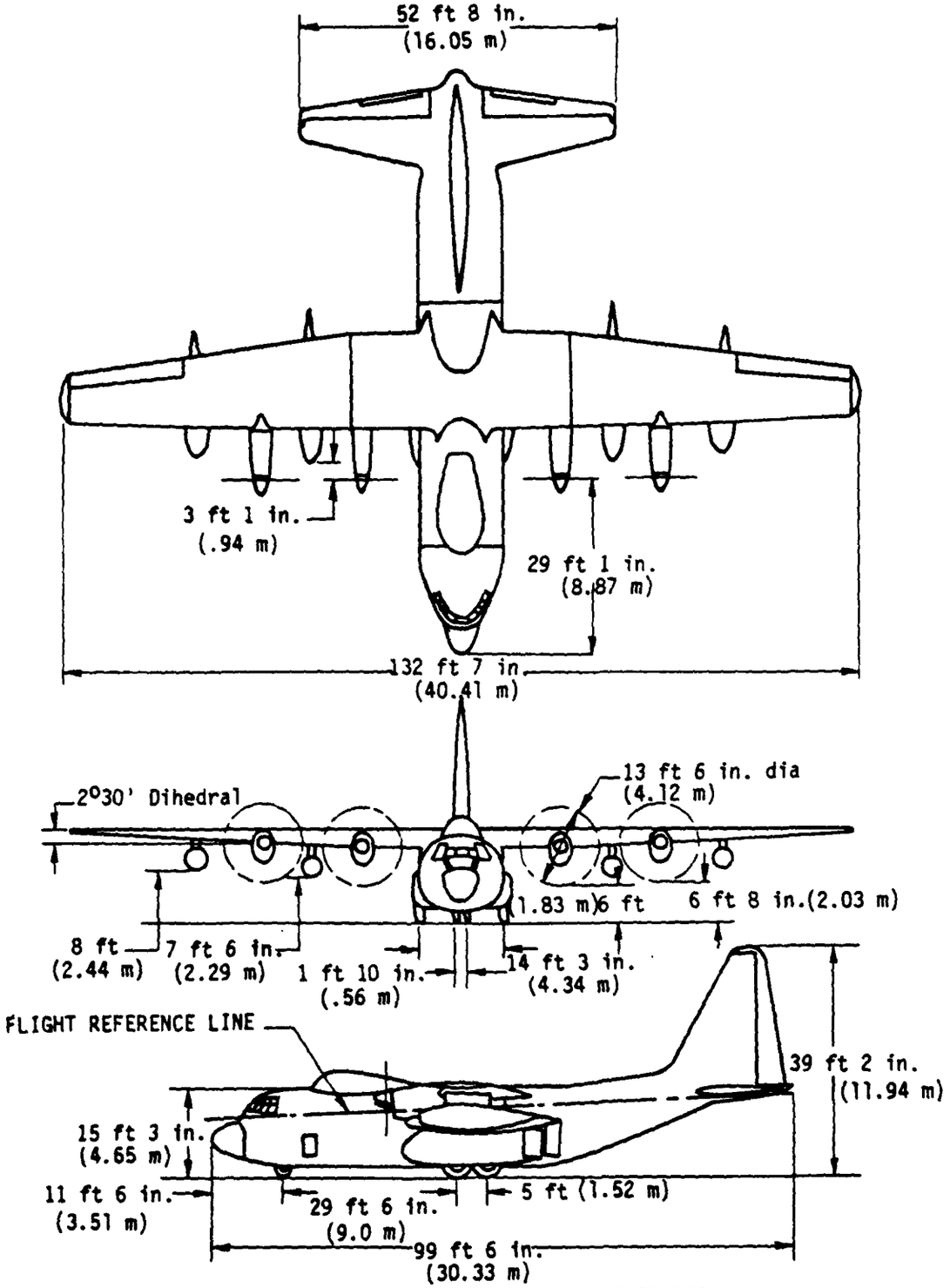

Figure A11. Principal dimensions of EC-130.

In order to obtain detailed information about the components/antennas under the fuselage, MRC made a trip to Dallas, Texas, where an EC-130 was located. Detailed data obtained by measurement of the aircraft is presented in figures.

The EC-130 studied was a G series, i.e., an EC-130G. The aircraft had only 100 gallons of fuel at the time the measurements were taken, so it was practically empty. It was observed that the front and the main wheel doors can be disconnected from the airplane if wanted. Figure A12 presents the dimensions of the front and the main landing gears in detail.

Figure A13 shows the EC-130G with its under-fuselage antennas which are indicated by letters from A to F on the figure. The front wheel door slides back, whereas the main wheel doors open to the sides. The tail skid shown on the figure is to protect the aft fuselage of the aircraft during the take-off and the landing.

The ground clearance of the external fuel tanks of the wings is 2.2 km. The minimum ground clearance of the inboard engine blades is 1.80 m.

Figure A14 shows the antenna/component dimensions under the fuselage of the EC-130G with their ground clearances. Note that this aircraft is the lowest (i.e., bottom of the fuselage is closest to the ground) of the three aircraft considered in EMP isolation study.

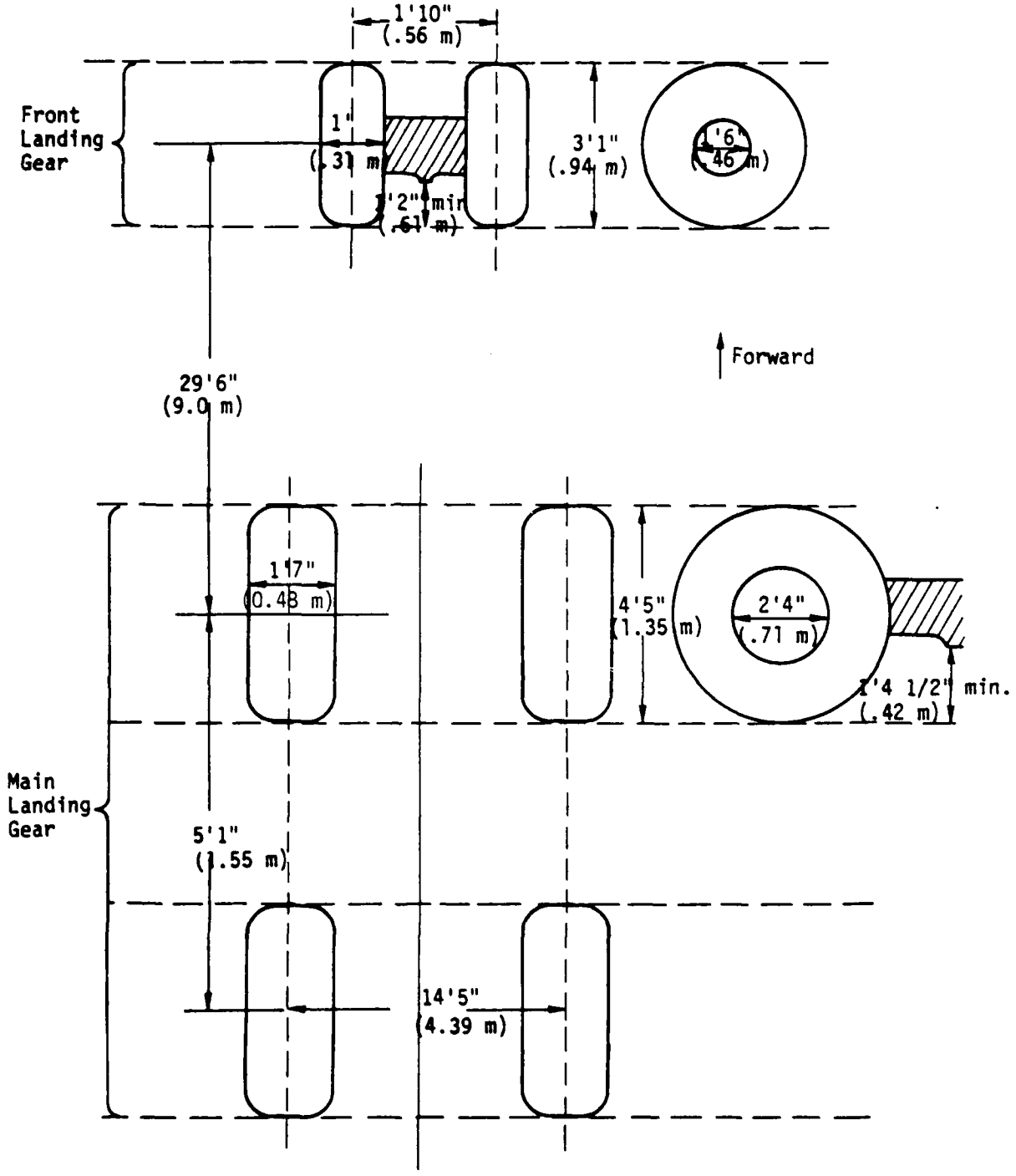

Figure A12. Front and main landing gears of EC-130G.

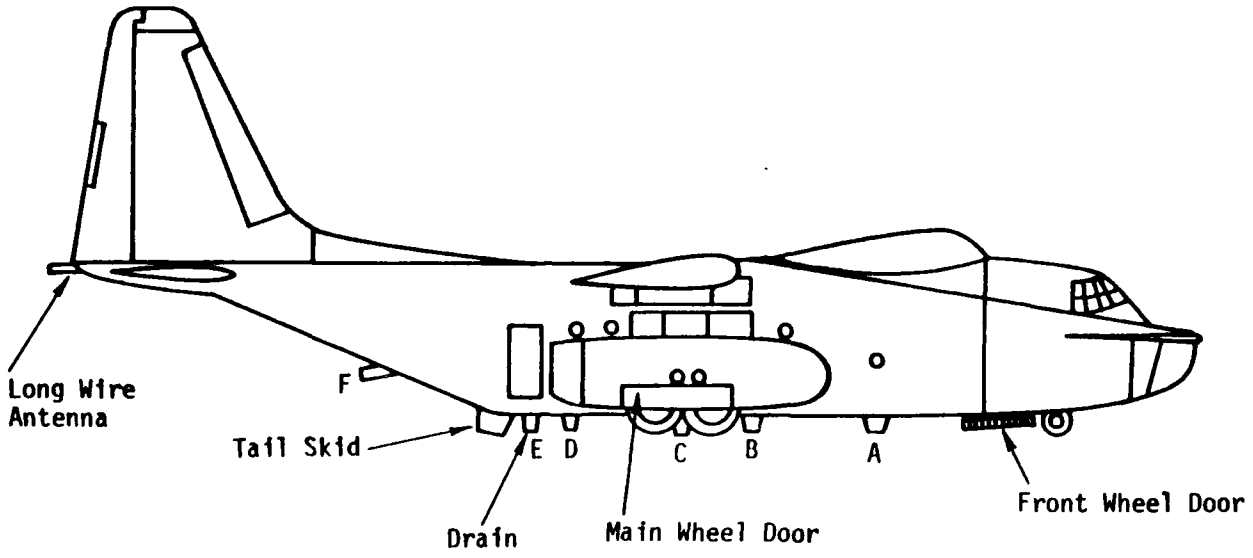

Figure A13. EC-130G antennas.

AD-A093 772 MISSION RESEARCH CORP ALBUQUERQUE NM F/G 20/14
AIRCRAFT EMP ISOLATION STUDY.(U)
JUL 80 A FINCI, H PRICE, P CHAO, S MERCER F29601-78-C-0082
UNCLASSIFIED AFWL-TR-79-156 NL

2 OF 2

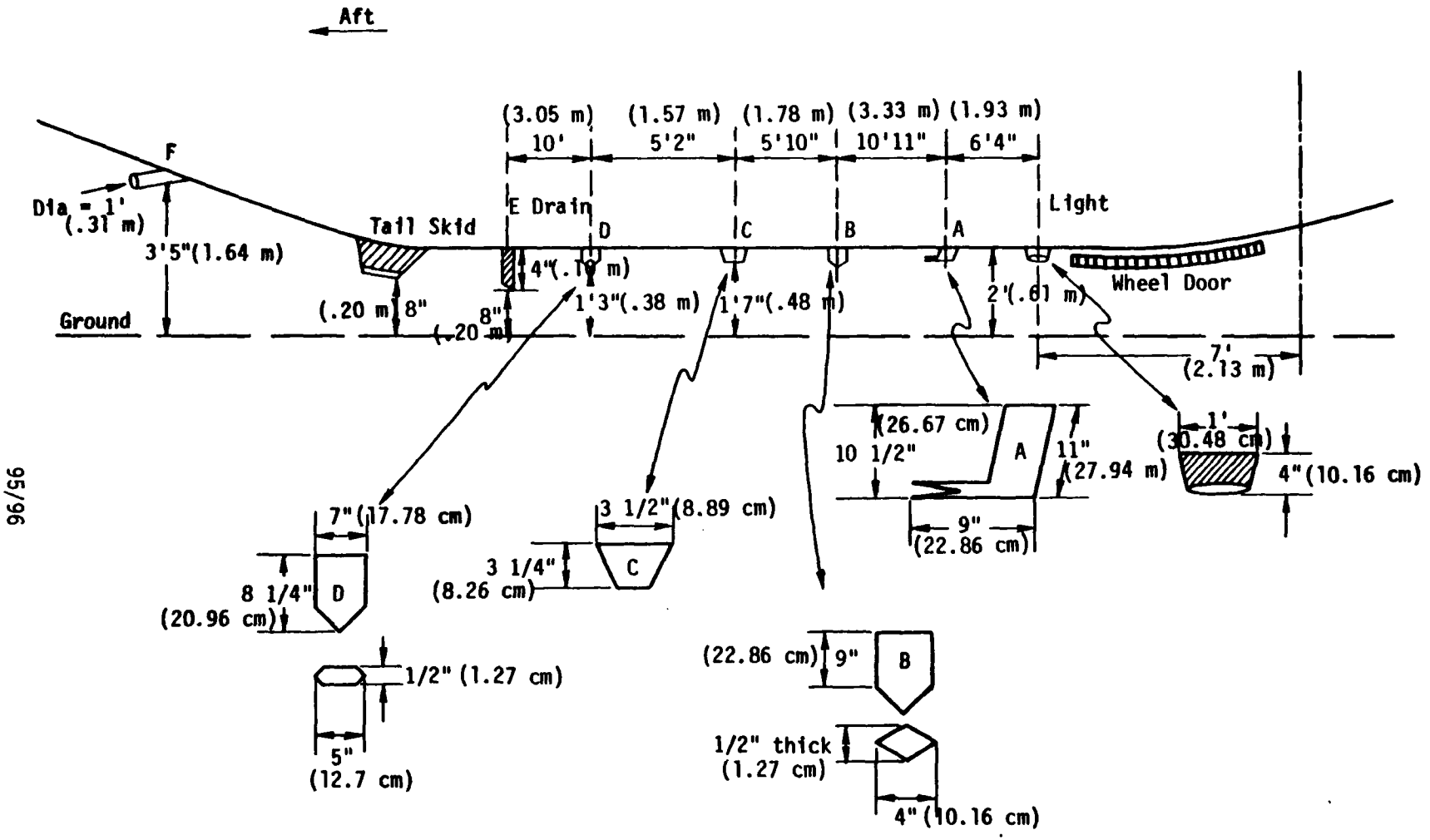

Figure A14. Antennas/components of EC-130G bottom fuselage.

95/96

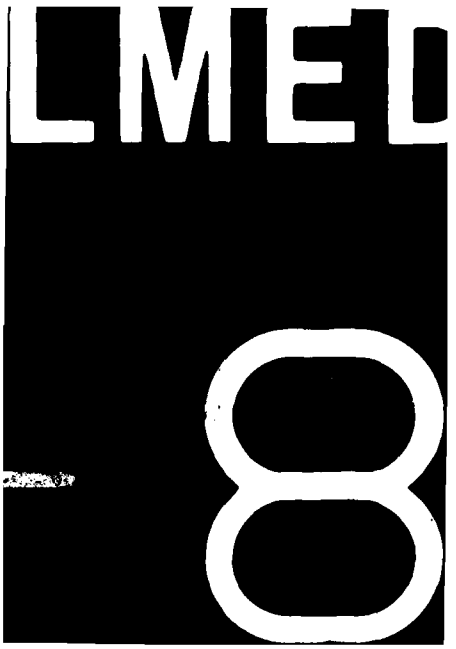
LMED
8